In Silico Study of Alizarin

By

Kavyasree.D

(14PPH006)

Thesis submitted to

Avinashilingam Institute for Home Science and Higher Education for Women,

Coimbatore - 641 043

In partial fulfilment of the requirements for the degree of

Master of Science in Physics

April, 2016

In Silico Study of Alizarin

By

Kavyasree.D

(14PPH006)

Thesis submitted to

Avinashilingam Institute for Home Science and Higher Education for Women,

Coimbatore - 641 043

In partial fulfilment of the requirements for the degree of

Master of Science in Physics

April, 2016

CERTIFIED AS A BONAFIDE RESEARCH WORK

29/4/16

Signature of the Head of the Department

29/4/16

Signature of the Guide

ACKNOWLEDGEMENT

ACKNOWLEDGEMENT

I owe my sincere thanks to **Lord Almighty** and **My Lovable Parents** without whom I would have been nothing and showering their generous blessings upon me in all endeavors.

I wish to express my profound sense of gratitude to **Dr.P.R.Krishnakumar,** Ph.D**.** Chancellor, Avinashilingam Institute for Home Science and Higher Education for Women, Coimbatore, for providing the facilities to conduct this study.

I extend my thanks to **Hon.Col. Dr.(Tmt.) Premavathy Vijayan, M.Sc., M.Ed., Dip.Spl.Edn., M.Phil., Ph.D,** Vice Chancellor (i/c), Avinashilingam Institute for Home Science and Higher Education for Women, Coimbatore, for providing flamboyant help towards the completion of the study.

I record my deep sense of gratitude and indebtedness to, **Dr. (Tmt.) A.Venmathi,** M.Sc, Dip.Ed, M.Phil, Ph.D. Registrar (i/c), Avinashilingam Institute for Home Science and Higher Education for Women, Coimbatore, for providing adequate help for the study.

I place on record my heartfelt thanks to **Hon.Col. Dr.(Tmt.) Saroja Prabakaran,** M.A., Dip.Ed., Ph.D., Former Vice Chancellor, The Director, Hall of Residence, Avinashilingam Educational Trust Institutions Hostel, Coimbatore, for extending all possible help towards the completion of the study.

I gratefully record my sincere thanks to **Dr. (Tmt.) A. Parvathi**, M.Sc., Dip. Ed., M.Phil., Ph.D., Dean, Faculty of Science, Avinashilingam Institute for Home Science and Higher Education for Women, Coimbatore, for timely help rendered throughout the course.

I would like to express my genial gratitude to **Dr.(Tmt.) J.Shanthi,** M.Sc., M.Phil., Ph.D., Associate Professor, Department of Physics, Avinashilingam Institute for Home Science and Higher Education for Women, Coimbatore, for her encouragement and generous help which was of great value.

I whole heartily thank my guide **(Tmt.) S.Anitha,** M.Sc., M.Phil., Assistant Professor, Department of Physics, Avinashilingam Institute for Home Science and Higher Education for Women, Coimbatore, for her encouragement, inspiring guidance, generous help, meticulous care and kind words in the time of need.

I sincerely thank **all the staff members** of the Department of Physics, Avinashilingam Institute for Home Science and Higher Education for Women, Coimbatore, for their help and support.

I also wish to thank **Dr. N.Shanthi**, **Assistant Professor and all staff members**, Department of Biochemistry, biotechnology and bioinformatics, Avinashilingam Institute for

Home Science and Higher Education for Women, Coimbatore, for their valuable help in completion of my project.

I would like to express my special thanks to **my friends** and all **my well wishers** for their constant encouragement, support and help in carrying out this work successfully.

KAVYASREE.D

CONTENT

CONTENT

LIST OF FIGURES

LIST OF TABLES

INTRODUCTION

CHAPTER I

INTRODUCTION

1.1 ALIZARIN

A Dihydroxy anthraquinone is an isomeric organic compound with formula C14H8O4, derived from 9, 10-anthraquinone by replacing two hydrogen atoms by hydroxyl groups. Hydroxyanthrequinones are a class of molecules which have attracted wide interest from both applied and fundamental point of view [1]. The dihydroxy-9,10-anthraquinone functional group occurs widely in natural products, and have important feature of the anthracycline anti-tumour antibiotics. 1,2-Dihydroxy-9,10-anthraquinone (Alizarin) is among the most important natural and synthetic compounds, which have found wide application as analytical reagent and indicator, biologically active agent and medicine, dye and intermediate product in the synthesis of dyes, chemical agent for data recording and storage material, etc [2]. The structure of Alizarin is shown in the fig: 1.1. Alizarin is the core moiety of Adriamycin, an important antitumor drug and had numerous applications owing to their interesting photo activity [3]. Hydroxyanthraquinone is known to be a good photosensitizer for photo dynamical therapy as an anti-tumor [4–6]. In particular, di-hydroxyanthraquinones have important application as a prominent family of pharmaceutically active and biologically relevant chromophores [7,8]. Many of them have been used as an analytical tool for the determination of metals, and in electrochemistry [9,10]. 1,2-dihydroxyanthraquinone (Alizarin-AZ) had numerous applications owing to their interesting photo activity. AZ is the core moiety of adriamycin, an important anti-tumor drug and have a remarkable antigenotoxic activity [11]. AZ is a component of food, which can act against the action of carcinogens and it is also used as a dye and chemical agent for data recording and storage material.

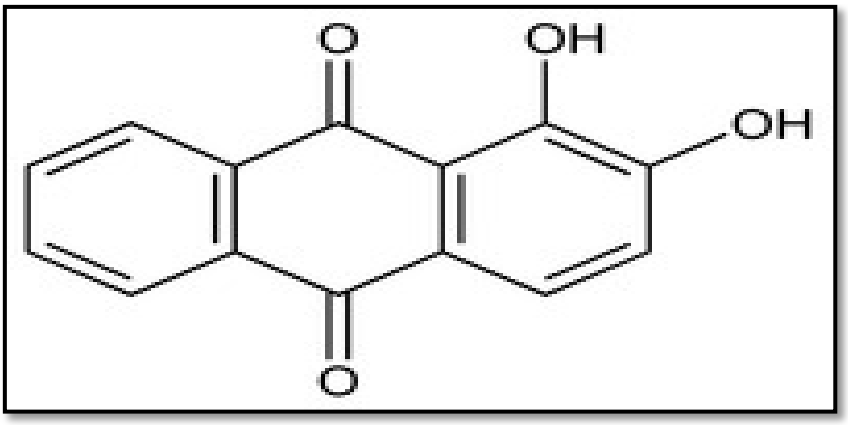

Fig: 1.1 Alizarin

1.2 SERUM ALBUMIN

Serum albumin is the most abundant blood plasma protein. It is produced in liver and forms a large proportion of all plasma protein. The human version is human serum albumin and it constitutes about 50% of human plasma protein [12]. Human Serum Albumin is encoded by ALB gene [13][14]. Other mammalian forms, such as Bovine Serum Albumin are chemically similar to human serum albumin. Serum albumin possesses a unique capability to bind covalently or reversibly with a great number of endogenous and exogenous compounds. Several different transport proteins exist in blood plasma but among that, albumin is the only protein able to bind with a wide diversity of ligands with high affinity.

Serum albumins play an important role in regulating blood volume by maintaining the oncotic pressure of the blood and also serve as carriers for molecules of low water solubility. The structure of Serum Albumin is shown in fig: 1.2.

1.3 BOVINE SERUM ALBUMIN

Serum Albumin has been one of the most extensively studied proteins for many years. It is the most abundant protein in blood plasma with a typical concentration of 50g/L. The main function of Serum Albumin is to transport protein for numerous endogenous and exogenous substances. It also plays an important role in regulating the colloid osmotic pressure of blood. Some of these albumins are Human Serum Albumin (HSA), Bovine Serum Albumin (BSA), Equine Serum Albumin (ESA) and Rat Serum Albumin (RSA). Serum Albumin has been a model protein for many years for physiological studies. BSA and HSA were the earliest primary sequences that were determined [15]. BSA has numerous biochemical applications including Enzyme-Linked Immunosorbent Assay and immunohistochemistry. BSA is used to stabilize some enzymes during digestion of DNA and to prevent adhesion of the enzyme to reaction tubes, pipet tips and other vessels [16]. BSA is used to determine the quantity of other proteins, by comparing an unknown quantity of protein to known amounts of BSA.

1.3.1 STRUCTURE OF BOVINE SERUM ALBUMIN

On the basis of the amino acid sequence, Brown proposed a 3-domain model for BSA. Brown proposed that BSA was composed of 582 amino acid residues. The sequence has 17 disulfide bonds resulting in nine loops formed by the bridges. BSA contains one single cysteine and eight pairs of disulfide bonds arranged in a way similar to those of HSA [17]. BSA also contains a high content of Asp, Glu, Ala, Leu and Lys residues which is analogous to HSA and RSA. The structure of BSA is composed of three homologous domains, (I, II,

AND III) which correspond to the residues 1-190, 191-382, 385-582 respectively. Each has about 190 residues, linked together by peptide chain and each domain can be subdivided into two subdomains, namely A and B. Domains I and II shows 25% identity, domains II & III and I & III show 21% and 18% identity respectively. Subdomains IA, IB and IIA pack tightly to form an enlarge head for the molecule whereas the extended tail is formed by subdomains IIB, IIIA and IIIB is shown in fig: 1.3 [18]. BSA and HSA share about 80% primary sequence identity with each other [19]. This result implies that BSA and HSA are homologous proteins which might have very similar biological functions. The most interesting property of serum albumin is the high affinity with various kinds of ligands or negatively charged molecules, which are located in different binding regions in serum albumins. The most outstanding feature of the albumin-ligand interactions is the presence of a few high affinity binding sites and a number of low affinity binding sites that interact with various kinds of ligands such as fatty acids, metals etc [20].

Fig: 1.2 Serum Albumin

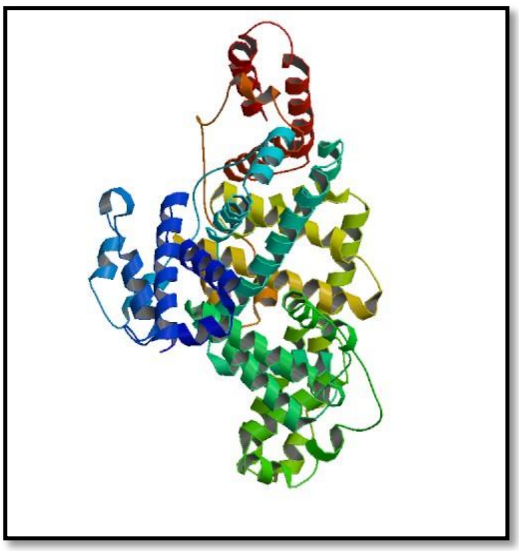

Fig: 1.3 Bovine Serum Albumin

1.4 AMINO ACIDS

Twenty percent of the human body is made up of protein. Protein plays a major role in almost all biological processes and amino acids are the building blocks of it. A large proportion of human cells, muscles and tissues are made up of amino acids and play an important role in the transport and the storage of nutrients. Amino acids are biologically important organic compounds containing amine ($-NH_2$) and carboxylic acid (-COOH) functional groups. The key elements present in an amino acid are carbon, hydrogen, oxygen, and nitrogen. Other elements are also found in the side-chains of certain amino

acids. About 500 amino acids are known and they can be classified in many ways [21]. The structure of amino acid is shown in fig: 1.4.

1.4.1CLASSIFICATION OF AMINO ACIDS

The amino acids involve in the formation of a peptide linkage with similar or different molecules. The peptide linkage is an amide bond that is formed by the condensation polymerization of amino group of one molecule and the carboxyl group of another molecule by eliminating water molecules. The amino acids with the presence of $–NH_2$ and –COOH called alpha amino acids, the side chain vary from molecule to molecule. The side chain effect the polarity of a molecule because $–NH_2$ and COOH on an alpha carbon atom can neutralize each other. On the basis of polarity, amino acids can be classified as:

- Polar amino acids
- Non polar amino acids

(a) POLAR AMINO ACIDS

Polar amino acids include Serine, Threonine, Asparagine, Glutamine, Histidine and Tyrosine. Polar amino acids can again classify as positively charged and negatively charged amino acids.

(a.1) POSITIVELY CHARGED AMINO ACIDS

Polar amino acid with positive charge has more amino groups as compared to carboxyl groups and becomes basic. The amino acids, which have positive charge on the 'R' group, belong to this category. Amino acids included in this group are Lysine, Arginine and Histidine.

(a.2) NEGATIVELY CHARGED AMINO ACIDS

Polar amino acids with negative charge have more carboxyl group than amino groups making them acidic. The amino acids, which have negative charge on the 'R' group, are placed in this category called as dicarboxylic mono-amino acids. Amino acids included in this group are Aspartic acid and Glutamic acid.

(b) NON POLAR AMINO ACIDS

Non polar amino acids have equal number of amino acids and carboxyl groups and they are neutral. These amino acids are hydrophobic and have no charge on the 'R' group. The amino acids in this group are Alanine, Valine, Leucine, Isoleucine, Phenyl Alanine, Glycine, Tryptophan, Methionine and Proline.

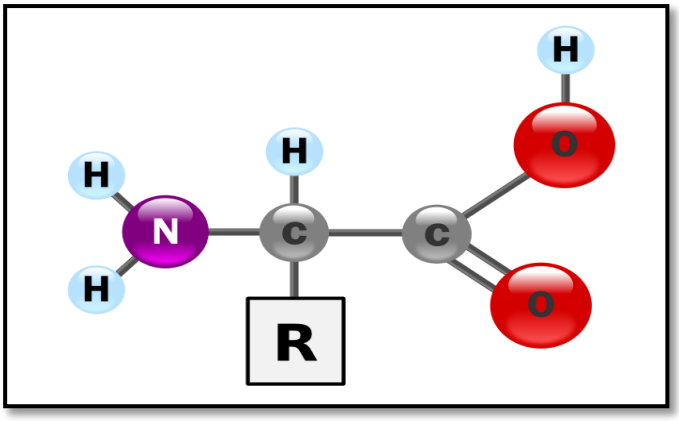

Fig: 1.4 Amino Acid

Name	Abbrev.	Structure*	Name	Abbrev.	Structure*
Alanine	Ala, A	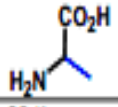	Leucine	Leu, L	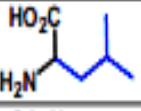
Arginine	Arg, R	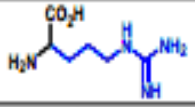	Lysine	Lys, K	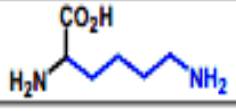
Asparagine	Asn, N	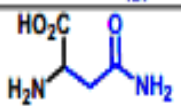	Methionine	Met, M	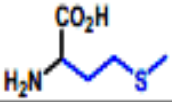
Aspartic Acid	Asp, D	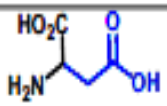	Phenylalanine	Phe, F	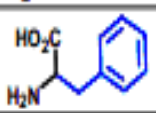
Cysteine	Cys, C	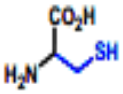	Proline	Pro, P	
Glutamic Acid	Glu, E	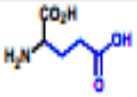	Serine	Ser, S	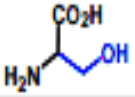
Glutamine	Gln, Q	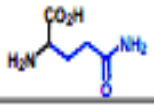	Threonine	Thr, T	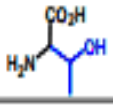
Glycine	Gly, G	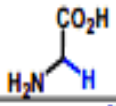	Tryptophan	Trp, W	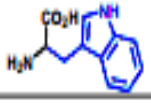
Histidine	His, H	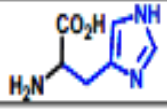	Tyrosine	Tyr, Y	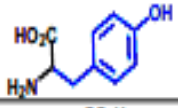
Isoleucine	Ile, I	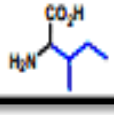	Valine	Val, V	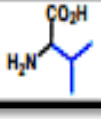

Fig: 1.5 Different types of amino acids

1.5 PROTEIN

Proteins are the primary structure and functional polymers in living systems. They have a broad range of activities, including catalysis of metabolic reactions and trans port of vitamins, minerals, oxygen and fuels. Some proteins make up the structure of tissues, nerve transmission, muscle contraction, cell motility, blood clotting and immunologic defense etc. Proteins are synthesized as a sequence of amino acids linked together and assume complex three dimensional shapes in performing their functions. There are about 300 amino acids present in various animals, plants and microbial systems, but only 20 amino acids are coded by DNA to appear in proteins. Proteins differ from one another primarily in their sequence of amino acids. A linear chain of amino acid residues called polypeptide. Short polypeptides, which contain less than 20-30 residues are rarely considered to be proteins and are called peptides. Proteins are essential parts of organisms and participate virtually in every process with in the cells. Proteins have structural or mechanical functions, such as actin, myosin in muscle and the proteins in the cytoskeleton, which form a system of scaffolding that maintains cell shape. Biochemists often refer to four distinct aspects of a protein's structure [22].

1.5.2 STRUCTURE OF PROTEIN

(A) PRIMARY STRUCTURE

The primary structure of a protein refers to the linear sequence of amino acids in the polypeptide chain. The primary structure is held together by covalent bonds such as peptide bonds, which are made during the process of protein biosynthesis or translation shown in fig: 1.5. The two ends of the polypeptide chain are referred to as the carboxyl terminus and the amino terminus based on the nature of the free group on each extremity. Counting of residues is started from the N-terminal end (NH_2 group) and ends with amino group. The sequence of a protein is unique, which defines the structure and function of the protein [23].

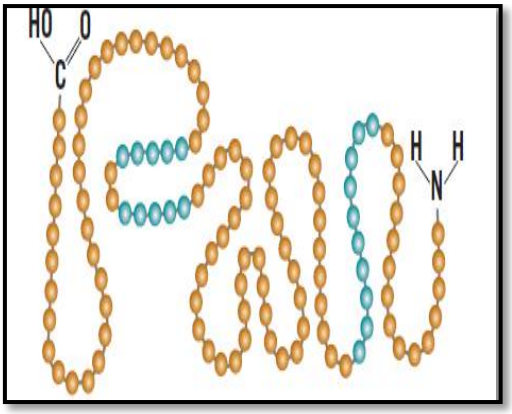

Fig: 1.5 Primary structure of protein

(B) SECONDARY STRUCTURE

Secondary structure refers to highly regular local sub - structures on the actual polypeptide back-bone chain, which have a regular geometry, being constrained to specific values of the dihedral angles ψ and ϕ on the Ramachandran plot. Two main types of secondary structure are the alpha helix and the beta strand or beta sheets. It is suggested by Linus Pauling and co-workers in 1951 [24]. The secondary structures are defined by patterns of hydrogen bonds between the main chain peptide groups. Both the alpha helix and the beta sheet represent a way of saturating all the hydrogen bond donors and acceptors in the peptide backbone.

(B.1) ALPHA HELIX

The alpha helix is a right handed coiled strand. The side chain substituent of the amino acid groups in an alpha helix extend to the outside. Hydrogen bond forms between the oxygen of C=O group of one amino acid and the hydrogen of the N-H group of the amino acid which is arranged in the form of helix is shown in fig: 1.7. The hydrogen bond makes the structure more stable. The side chain substituent of the amino acids fit in beside the N-H groups.

(B.2) BETA SHEET

Hydrogen bonds are formed between peptide bonds in different chains; the chains become arrayed parallel or antiparallel to one another, called a beta pleated sheet or beta strand as shown in fig: 1.8. The antiparallel beta sheet is more stable due to the well aligned hydrogen bonds.

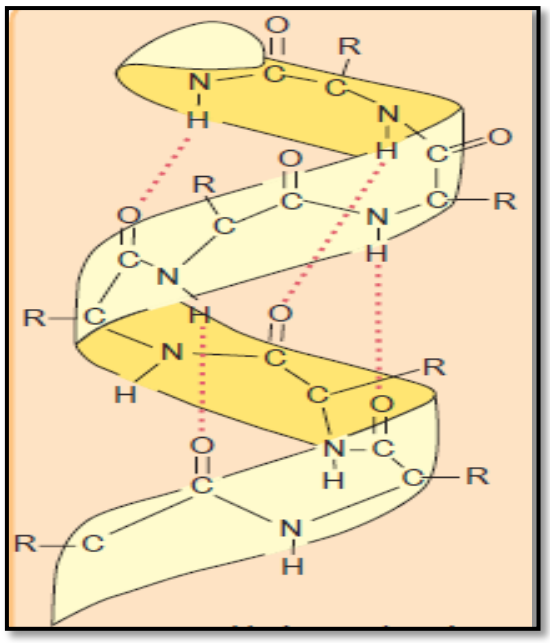

Fig: 1.7 Alpha helix

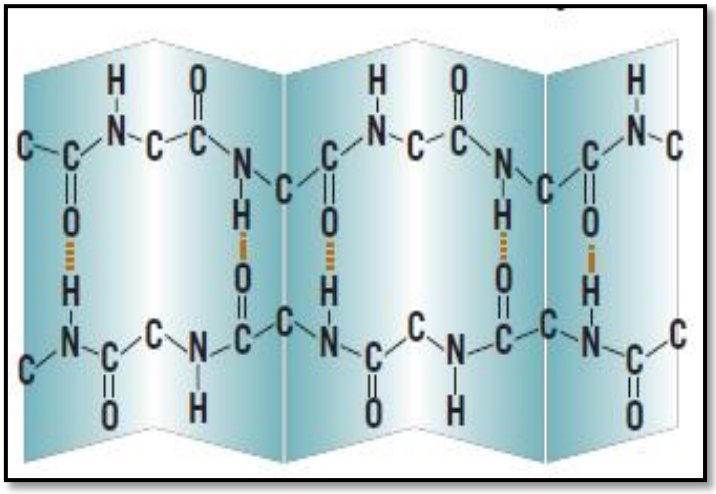

Fig: 1.8 Beta sheet

(C) TERTIARY STRUCTURE

The overall three dimensional shape of an entire protein molecule is the tertiary structure. The protein molecule will bend and twist in such a way as to achieve maximum stability or lowest energy state as shown in figure: 1.9. The three dimensional shape of a protein is irregular, random, and fashioned by many stabilizing forces due to bonding interactions between the side chain groups of the amino acids. The three dimensional tertiary structure of a protein is stabilized by interactions between side chain functional groups: covalent disulfide bonds, hydrogen bonds, salt bridges and hydrophobic interactions [25].

(D) QUATERNARY STRUCTURE

Many proteins are made up of multiple polypeptide chains, often referred to as protein subunits, which may be same in homodimer or different in heterodimer. The quaternary structure refers to protein subunits interact with each other and arrange themselves to form a large aggregate protein complex. Fig: 1.10 shows the Quaternary structure of protein.

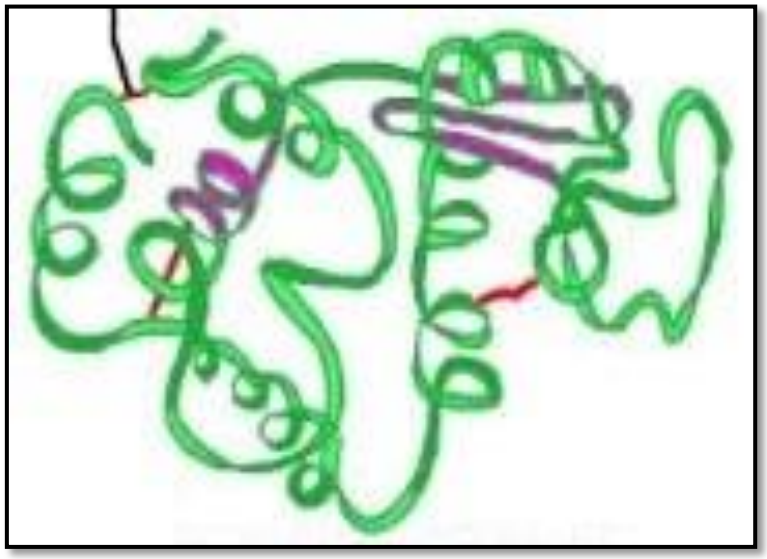

Fig: 1.9 Tertiary Structure

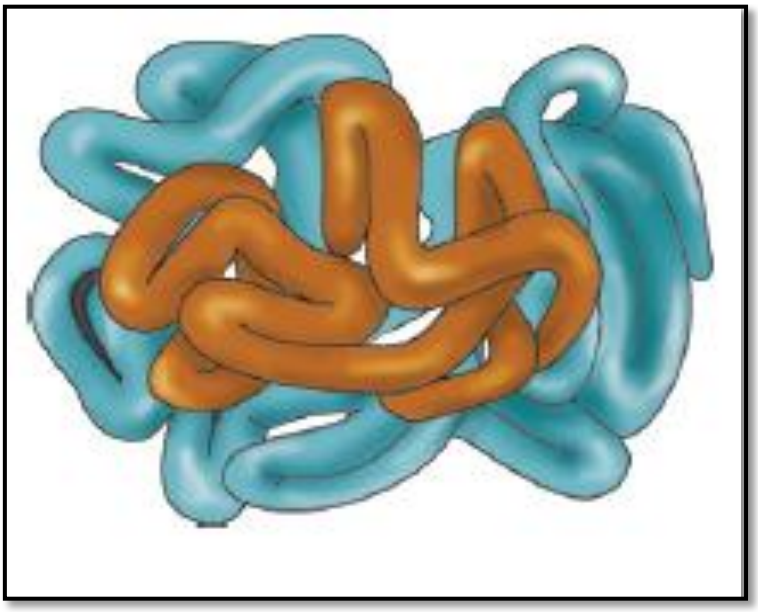

Fig: 1.10 Quaternary Structure

1.6 TYPES OF MOLECULAR BONDS

1. Covalent bond
2. Ionic bond
3. Hydrogen bond

1.6.1 COVALENT BOND

Covalent bond is a chemical bond that involves the sharing of electron pairs between atoms. The stable balance of attractive and repulsive forces between atoms is due to sharing of electrons as shown in fig: 1.11 [26]. For many molecules, the sharing of electrons allows each atom to attain the equivalent to a full outer shell, corresponding to a stable electronic configuration. Covalent bonding includes many kinds of interactions, including π-bonding, σ-bonding, metal-to-metal bonding, bent bonds etc [27][28]. The term covalent bond dates from 1939 [29]. In H_2 molecule, the hydrogen atoms share the two electrons via covalent bonding [30]. Covalence is greatest between atoms of similar electro-negativities and does not require that the two atoms be of the same elements, only it may be of comparable electro- negativity. Covalent bonding that entails sharing of electrons over more than two atoms is to be delocalized.

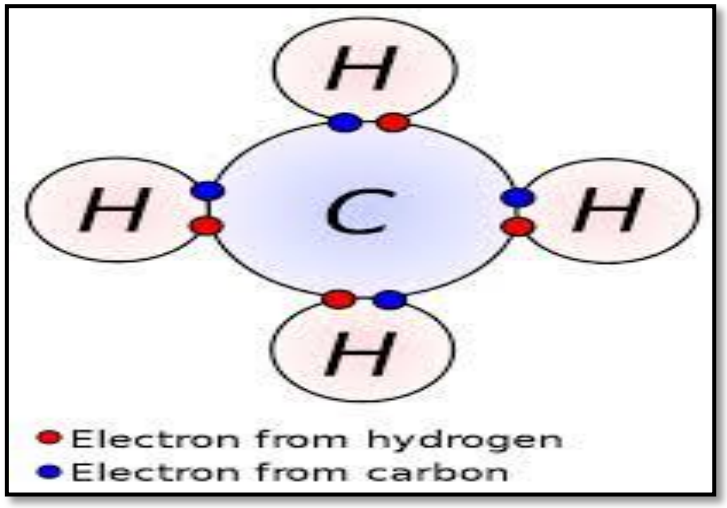

Fig: 1.11 Covalent bond

1.6.2 IONIC BOND

Ionic bond is a type of chemical bond that involves the electrostatic attraction between oppositely charged ions. The ions are atoms, which have lost one or more electrons are cations and atoms that have gained one or more electrons are anions. Fig: 1.12 shows the ionic bond. Transfer of electrons is electrovalence, in which the cation is

a metal atom and the anion is a non metal atom. An ionic bond is the transfer of electrons from a metal to a non metal in order to obtain a full valence shell.

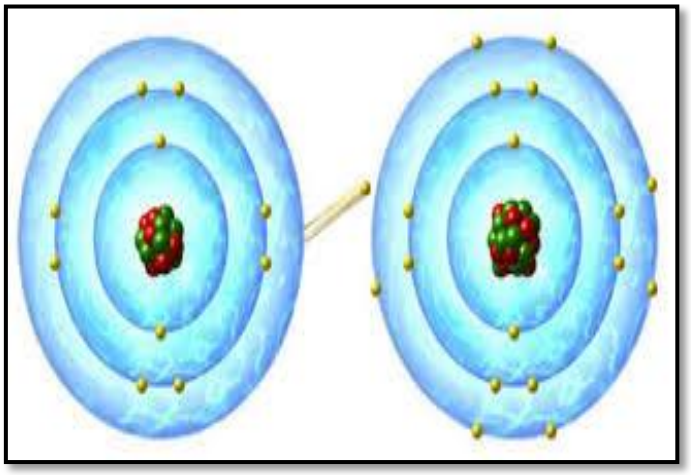

Fig: 1.12 Ionic bond

1.6.3 HYDROGEN BOND

Hydrogen bond is the electrostatic attraction between polar groups that occurs when hydrogen (H) atom bound to a highly electronegative atom such as nitrogen (N), oxygen (O) or fluorine (F). Figure: 1.13 shows the Hydrogen bond attractions. It can occur between molecules or within different parts of a single molecule [31]. Depending on geometry and environmental conditions, the hydrogen bond may be worth between 5 and 30 KJ/ mole in thermodynamic terms. This makes it stronger than a Van der Waals interaction, but weaker than covalent or ionic bonds. This type of bond can occur in inorganic molecules such as water and in organic molecules, like DNA and proteins.

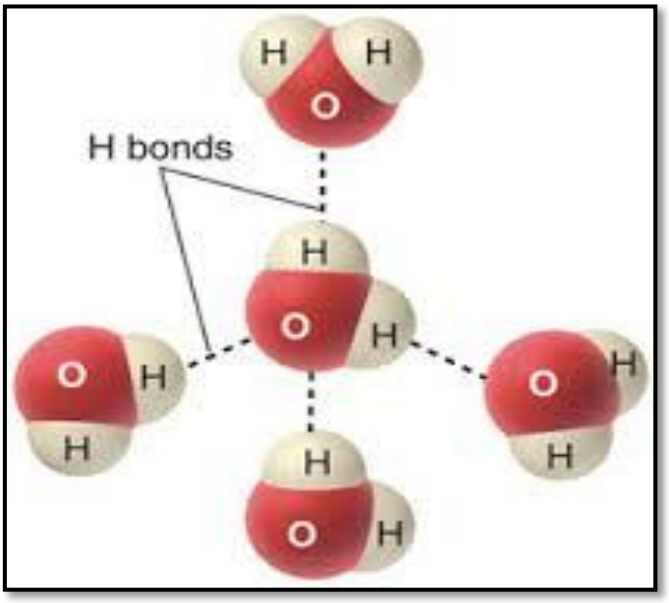

Fig: 1.13 Hydrogen bond

1.7 OBJECTIVE OF THE PRESENT WORK

The main objective of the present study is:

- To optimize the structure of Alizarin and Alizarin with different solvents by using GAUSSIAN 09 program.
- UV-VIS, NMR, IR and Raman spectra were analyzed.
- To dock the ligand Alizarin with Bovine Serum Albumin (BSA) using maestro Schrödinger software.

1.8 REFERENCES

[1] Anslyn, Eric (2004). Modern Physics Organic chemistry. Sausalite CA; University Science. Page: 978-1-891389-31-3.

[2] Fain V Y, Zaitsev B E, Ryabov M A (2004). Quantum- Chemical and Correlation Study of Ionization of Alizarin. Russ J Gen Chem 7, page: 1558-63.

[3] Fain, V.Ya (1999), 9, 10-Antrakhinony i ikh primenenie; 9, 10-Anthraquinones and their application, Moscow: Tsentr Photokhimii Ross. Akad. Nauk.

[4] J. R. Choi, S. C. Jeoung, D. W. Cho, Chem. Phys. Lett. 385 (2004) 384.

[5] T.D. Giacco, L. Latterini, F. Elisei, Photochem. Photobiol. Sci. 2 (2003) 681.

[6] C. Milliani, A. Romani, G. Favaro, J. Phys. Org. Chem. 13 (2000) 141.

[7] S.H. Cho, H. Huh, H.M. Kim, C.I. Kim, N.J. Kim, S.K. Kim, J. Chem.Phys.122 (2005).

[8] M.P. Marzocchi, A.R. Mantini, M. Casu, G. Smulevich, J. Chem. Phys.108 (1998) 534.

[9] M.V. Canamares, J.V.G. Ramos, C. Domingo, S.S. Cortes, J. Raman Spectrosc.35 (2006), 921.

[10] Nelson DL, Cox MM (2005) "Lehninger's Principles of Biochemistry" (4th ed.) New York: W.H.Freeman and Company.

[11] Gutteridge A, Thornton JM (2005) "Understanding nature's catalytic toolkit" Trends in Biochemical Sciences 30 (11): page: 622-29.

[12] Farrugia Albert (January 2010) "Albumin Usage in Clinical Medicine: Tradition or Therapeutic?" Transfusion Medicine Reviews 24 (1): page: 53-63.

[13] Hawkins JW, Dugaiczyk A (1982) "The human serum albumin gene: structure of a unique locus" Gene 19 (1): page: 55-8.

[14] Harper ME, Dugaiczyk A (July 1983) "Linkage of the evolutionarily-related serum albumin and alpha-fetoprotein genes within q11-22 of human chromosome 4" Am.J.Hum.Genet 35 (4): page: 565-72.

[15] Behrens P.Q, Spiekerman A.M and Brown J.R (1975) " Structure of Human Serum Albumin" Fedeartion Proceedings 34: page: 591

[16] " BSA FAQ " Invitrogen. Retrieved 19 January 2012.

[17] He X.M and Carter D.C (1992) "Atomic Structure and Chemistry of Human Serum Albumin" Nature 358: page: 209-215.

[18] Carter D.C, He X.M, Munson S.H, Twigg P.D, Gernert K.M, Broom M.B and

Miller T.Y (1989) " Three-Dimensional structure of Human Serum Albumin " Science 244: page: 1195-1198.

[19] Peters, T. Jr (1985) "Serum Albumin" Advances in Protein Chemistry 37: page: 161-245.

[20] Kragh-Hansen U (1981) " Molecular Aspects of Ligand Binding to Serum Albumin " Pharmacological Reviews 33 (1): page: 17-53.

[21] Pauling L, Corey R B, Branson H R (1951) "The structure of protein; two hydrogen-bonded helical configurations of the polypeptide chain" Proc Natl Acad Sci USA 37 (4): page: 205-211.

[22] Bret A Shirley, "Protein Stability and Folding, Theory and Practice, Methods in Molecular Biology", Vol.40.

[23] Campbell, Neil A, Brad Williamson, Robin J Heyden (2006) "Biology: Exploring Life" Boson, Massachusetts: Pearson Prentice Hall.

[24] March, Jerry (1992) "Advanced organic chemistry: reactions, mechanisms and structure" John Wiley & Sons.

[25] Gary L Miessler, Donald Arthur Tarr (2004) "Inorganic chemistry" Prentice Hall.

[26] Merriam-Webster- Collegiate Dictionary (2000).

[27] IUPAC, Compendium of Chemical Terminology, 2nd ed (the "Gold Book") (1997) Online corrected version: (2006-).

[28] Vankar P.S, Shanker R, Mahanta D, Tiwari S C (2008) "Ecofriendly Sonicator Dyeing of Cotton with Rubia cordifolia Linn Using Biomordant" Dyes and Pigments 76 (1): page: 207-212.

[29] Bien H S, Stawitz J, Wunderlich K (2005) "Anthraquinone Dyes and Intermediates" Weinheim: Wiley-VCH.

[30] J P Srivastava (2006) "Elements of solid state physics" Prentice hall of India (P) Ltd; page: 37.

[31] Anslyn, Eric (2004) "Morden Physics Organic Chemistry" Sausalite CA; University Science.

REVIEW OF LITERATURE

CHAPTER 2
REVIEW OF LITERATURE

2.1 INTRODUCTION

Review of the related literature is an essential part of research project. The research carried out on the topics related to the in silico study of Alizarin and molecular docking studies of Alizarin with Bovine Serum Albumin (BSA) was briefly recorded in this chapter.

[1] V. SASIREKHA et al (2008) studied the preferential solvation of a solvatochromic probe in binary mixtures comprising of a non-protic and a protic solvent. The non-protic solvents employed are carbon tetrachloride (CCl4), acetonitrile (AcN) and *N*,*N*-dimethyl formamide (DMF) and the protic solvents are methanol (MeOH) and ethanol (EtOH). The probe molecule exhibits different spectroscopic characteristics depending upon the properties of the solubilising media. The observed spectral features provide an indication of the microenvironment immediately surrounding the probe. Solvatochromic shifts of the ground and excited states of the probe were analysed by monitoring the charge transfer absorption band and the fluorescence emission spectra in terms of the solute–solvent and solvent–solvent interactions. Fluorescence emission spectra show the dual emission due to excited state proton transfer nature of the probe molecule. The effect of solvent and the excitation energy on dual emission are also studied. The observed magnitude of the Stokes shift in the above solvents has been used to deduce experimentally the dipole moment ratio of the probe molecule for the excited state to the ground state. The dipole moment of excited state is higher than the ground state.

[2] ZAHRA VARMAGHANI at el (2014) have optimized Vinblastine in vacuum and then in different solvents by Density Functional Theory (DFT) method. Nuclear Magnetic Resonance (NMR) shift measurements were made in different solvents by various dielectric constants by continuous set of Gauge Transformations (CSGT). The result shows the best structure and function of vinblastine. The conformational preferences attributed to the stereo-electronic effect. The results showed that the structure of vinblastine is more stable in water rather than the other media. The most active atoms of vinblastine were realized by various spectra of vinblastine in different media including vacuum and diverse solvents. The

active site of vinblastine that could bind to tubulin to perform the antimitosis and anticancer effect in process of cell division was also discovered.

[3] PRITHA GHOSH et al (2013) have studied the interactions of a few anthraquinone derivatives such as 1,2-dihydroxyanthraquinone (alizarin), 1,4-dihydroxyanthraquinone (quinizarin), 1,8-dihydroxy anthraquinone (danthron), 1,2,4-trihydroxyanthraquinone (purpurin), 1,4-diaminoanthraquinone, and 1-methylamino anthraquinone for its possible interaction with calf-thymus DNA through spectroscopy and in silico analysis. Anthraquinones consist of several hundreds of derivatives that differ in the nature and positions of substituent groups which have several biological activities including antitumor properties. The UV spectroscopic results indicate that all the selected anthraquinones interact with DNA probably by external binding. Molar extinction coefficient has been calculated for chosen six anthraquinones. Among the six dyes used, purpurin showed better results and indicates the relatively strong binding affinity with DNA. Molecular modeling results also show that purpurin has comparatively higher DNA interaction with a score of −6.18 compared with the ethidium bromide of −5.02 and intercalate the DNA.

[4] SABITHA KESAVAN et al (2015) have studied about the inhibitors that are bounded with Acrosin binding protein (ACRBP/OY-TES-1) through In silico molecular docking studies. Food and Drug Administration (FDA)-approved drugs were docked with ACRBP/OY-TES-1 to identify potent inhibitors. Molecular docking was applied to explore the binding mechanism of ACRBP/OY-TES-1 with FDA-approved drugs. Results indicate that peptides have a better binding affinity towards ACRBP/OY-TES-1. Docking calculations were carried out using Glide. Glide Score (GS core) was used to rank the ligands on the basis of their relative binding affinities. The Glide score for Leuprolide a decapeptide on interacting with the protein at residues Tyr116, Gly421, Leu433, Asp480 and Gln483 is 14.188. Other compounds that showed high affinity to the protein are triptorelin, nafatarelin, goserelin and sincalide.

[5] YUTING HU et al (2014) have examined the combination of fluorescence, UV–Vis absorption, circular dichroism (CD), Fourier transform infrared (FT-IR) and molecular modeling approaches to determine the interaction between lysionotin and bovine serum albumin (BSA) at physiological pH. The fluorescence titration suggested that the fluorescence quenching of BSA by lysionotin was a static procedure. The binding constant at

298 K was in the order of 10^5 L mol^{-1}, indicating that a high affinity existed between lysionotin and BSA. The thermodynamic parameters obtained at different temperatures (292, 298, 304 and 310 K) showed that the binding process was primarily driven by hydrogen bond and van der Waals forces, as the values of the enthalpy change ($\Delta H°$) and entropy change ($\Delta S°$) were found to be -40.81 ± 0.08 kJ mol^{-1} and -35.93 ± 0.27 J mol^{-1} K^{-1}, respectively. The surface hydrophobicity of BSA increased upon interaction with lysionotin. The site markers experiments revealed that the binding site of lysionotin was in the sub-domain IIA (site I) of BSA. Furthermore, the molecular docking results corroborated the binding site and clarified the specific binding mode. The results of UV–Vis absorption, CD and FT-IR spectra demonstrated that the secondary structure of BSA was altered in the presence of lysionotin.

[6] RAN MI et al (2013) have studied the interaction between jatrorrhizine (JAT) and bovine serum albumin (BSA). The studies were carried out in a buffer medium at pH 7.4 using fluorescence spectroscopy, UV–vis spectroscopy, and molecular modeling methods. The results of fluorescence quenching and UV–vis absorption spectra experiments indicated the formation of the complex of BSA–JAT. Binding parameters were determined using the Stern–Volmer equation and Scatchard equation. The results of thermodynamic parameters ΔG, ΔH and ΔS at different temperatures indicate that the electrostatic interactions and hydrogen bonds play a major role for JAT–BSA association. Site marker competitive displacement experiments and molecular modeling calculation showed that JAT is mainly located within the hydrophobic pocket of the subdomain IIIA of BSA. Furthermore, The distance between donor (BSA) and acceptor (JAT) had estimated according to fluorescence resonance energy transfer.

[7] HAO TANG et al (2015) examined the binding abilities of scutellarin (Scu) and scutellarein (Scue) with bovine serum albumin (BSA) using equilibrium dialysis, high performance liquid chromatography, fluorescence spectroscopy, competitive site marker and molecular docking. The results showed that the average protein binding ratios of Scu and Scue with BSA were (79.85 ± 1.83) and (85.49 ± 1.21) % respectively. The thermodynamic parameters indicated that the interactions of Scu-BSA and Scue-BSA mainly occurred by van der Waals forces and hydrogen bonds and it was easier for Scue to bind with BSA than Scu, indicating that the glucuronic acid molecule in Scu decreased the binding affinity. Site competitive marker experiments showed that the binding sites of Scu and Scue mainly

located within the sub-domain IIA of BSA. Furthermore, molecular docking studies indicated that one BSA could bind three Scue, while one BSA could carry only two Scu.

[8] XIAODI NIU et al (2013) have study, the binding of Bovine serum albumin (BSA) with three flavonoids, kaempferol-3-*O*-a-L-rhamnopyranosyl-(1–3)-a-L-rhamnopyranosyl-(1–6)-b-D-galacto-pyranoside (drug-1), kaempfol-7-*O*-rhamnosyl-3-*O*-rutinoside (drug-2) and kaempferide-7-O-(4”-*O*-acetylrhamnosyl)-3-*O*-ruti- noside (drug 3) is investigated by molecular docking, molecular dynamics (MD) simulation, and binding free energy calculation. The free energies are consistent with available experimental results and suggest that the binding site of BSA-drug1 is more stable than those of BSA-drug2 and BSA-drug3. The energy decomposition analysis had performed and it reveals that the electrostatic interactions play an important role in the stabilization of the binding site of BSA-drug1 while the van der Waals interactions contribute largely to stabilization of the binding site of BSA-drug2 and BSA-drug3. The key residues stabilizing the binding sites of BSA-drug1, BSA-drug2 and BSA-drug3 were identified based on the residue decomposition analysis.

[9] HAI WU at el (2011) have used a novel electrochemical site marker competitive method for the study of the binding site and the binding mode between bovine serum albumin (BSA) and alizarin red S (ARS). Two known site-selective markers for BSA, bilirubin (BR, for site I) and diazepam (DIA, for site II), were selected to bind to the two potential binding sites of BSA (site I and site II). The resulting BR–BSA or DIA–BSA complex had added into an ARS solution for binding site competition studies. From the current response of ARS after site competition, binding site I of BSA is identified as the binding site of BSA to ARS. Further investigation of the binding events by electrochemistry, fluorescence, and molecular docking techniques revealed that ARS had buried in the hydrophobic cavity of subdomain IIA, mainly through five hydrogen bonds between ARS and residues ARG(193), ARG(255), LYS(220), ARG(197), and ALA(289) of BSA.

[10] EBRAHIM BALALI (2014) have performed Quantum-mechanical calculations at the HF/6-31G, HF/6-31G*, B3LYP/6-31G, B3LYP/6-31+G, B3LYP/6-31G* and BLYP/6-31G** levels in the gas phase and four solvents such as water, DMSO, methanol and dichloromethane. According to these theoretical results, thermo chemical parameters such as energy of the whole system, enthalpy, Gibbs free energy and entropy for Tripeptide Tyr-Aaa-Gly were extracted. The results revealed that parameters are strongly affected by inducing different solvent media. According to these theoretical results it was concluded that the

dielectric permittivity of the solvent is a key factor that determines the chemical behavior of Tripeptide Tyr-Aaa-Gly in solution.

[11] AMMAR A. IBRAHIM and ROSIYAH YAHYA (2011) have evaluated the theoretical calculations for different solvents in the gas phase by semi-empirical using (PM3) method and ab initio calculations using both HF/3-21G and DFT/B3LYP/3-21G methods. The physical properties of these solvents were compared between them to choose the best solvent to dissolve the [phthalic anhydride-chitosan] monomer, (I). These solvents are: dimethylsulfoxide, N,N-dimethyl formamide, tetrahydrofuran, 1,2-ethylene diamine, ethylene-carbonic acid and propylene-carbonic acid. The calculations shows that (dimethylsulfoxide, N,N-dimethyl formamide and 1,2-ethylene diamine) are the good solvents to dissolve the [phthalic anhydridechitosan] monomer, (I). The physical properties of the formation of [phthalic anhydride-chitosan] monomer, (I), were also calculated, using the parameters: dipole moment, HOMO, LUMO, hardness (h), electronic chemical potential (μ) and global electrophilicity index (w). It had observed that the computed geometrical parameters using the (PM3), (HF/3-21G) and (DFT/B3LYP/3-21G) are in good agreement with the experimental and the parameters play an important role to choose the best solvent. The synthesized N-phthaloyl chitosan polymer had also dissolved in many solvents in order to study the effect of solvent experimentally, but only three organic solvents (dimethylsulfoxide, N,N-dimethyl formamide and 1,2-ethylene diamine) were found to be able to dissolve it. These results are in agreement with the theoretical calculations. Finally, these calculations are useful for choosing the best solvent to dissolve the polymer of [phthali canhydride-chitosan] monomer, (I).

[12] M. KANDASAMY at el (2013) have observed the vibrational spectroscopic of 9-fluorenone-2-carboxylic acid (9F2CA) by means of quantum chemical calculations. Comprehensive theoretical and experimental FTIR and FT-Raman spectral analysis of 9F2CA have been carried out by using DFT/B3LYP method with 6-31G(d,p) basis set. The equilibrium molecular geometry, harmonic vibrational frequencies, infrared and Raman intensities of 9F2CA have been calculated. The calculated vibrational spectrum had compared with the experimental data which provides reliable assignments of all observed bands in FTIR and FT-Raman spectra, including in the low frequency region. The ^{1}H and ^{13}C nuclear magnetic resonance (NMR) chemical shifts of the molecule were calculated by GIAO method and compared with available experimental data. Complete NBO analysis had also

carried out to find out the intramolecular electronic interactions and their stabilization energy. Also, the highest occupied molecular orbital (HOMO) and lowest unoccupied molecular orbital (LUMO) energies were found.

[13] A. SUVITHA at el (2015) have recorded the vibrational spectral by using Raman and infrared spectroscopy in the range 100–4000 cm_1and 50–4000 cm_1, respectively, for 2,2,4-Trimethyl Pentane, TMP (C8H18) molecule. The molecular structure, fundamental vibrational frequencies and intensity of the vibrational bands are interpreted with the aid of structure optimizations and geometrical parameter calculations based on Hartree Fock (HF) and density functional theory (DFT) method with 6-311++G (d,p) basis set. The scaled B3LYP/6-311++G (d,p) results shows the best agreement with the experimental values over the other method. The HOMO and LUMO energies were also calculated. The physical reactions of single bond hydrocarbon TMP were investigated. The results of the calculations were applied to simulate spectra of the title compound, which shows the excellent agreement with observed spectra. Besides, Mulliken atomic charges, UV, frontier molecular orbital (FMO), MEP, NLO activity, Natural Bond-Orbital (NBO) analysis, NMR and thermodynamic properties of title molecule were also performed.

2.2 REFERENCES:

[1] V. Sasirekha a, M. Umadevi b, V. Ramakrishnan; Solvatochromic study of 1,2-dihydroxyanthraquinone in neat and binary solvent mixtures; Spectrochimica Acta Part A 69 (2008), pages 148–155.

[2] Zahra Varmaghani, Majid Monajjemi, Fatemesh Mollaamin; Discovery Of Active Site Of Vinblastine As Application Of Nanotechnology In Medicine; Nanomedical Journal; Vol 1, No.3, pages 162-170.

[3] Pritha Ghosh, G. Poornima Devi, R. Priya, A. Amrita, A. Sivaramakrishna, S. Babu, R. Siva; Spectroscopic and In Silico Evaluation of Interaction of DNA with Six Anthraquinone Derivatives; Volume 170, Issue 5, July 2013,pages 1127-1137.

[4] Sabitha Kesavan, Priya Ramanathan, Rajkumar Thangarajan; Molecular Modelling And Docking Studies Of Human Acrosin Binding Protein (Acrbp/Oy-Tes-1); Vol 7, Issue 9, 2015.

[5] Yuting Hu, Guowen Zhang, Jiakai Yan; Detection of interaction between lysionotin and bovine serum albumin using spectroscopic techniques combined with molecular modeling; Volume 41, Issue 3, March 2014, pages 1693-1702.

[6] Ran Mi, Pei-Qi Li, Yan-Jun Hu, Xiao-Yang Fan, Hai-Ying Li, Xue-Cheng Yu, Yu Ouyang; Biophysical studies on the interactions of jatrorrhizine with bovine serum albumin by spectroscopic and molecular modeling methods; Volume 40, Issue 7, July 2013, pages 4397-4404.

[7] Hao Tang, Zhi-Hao Shi, Nian-Guang Li, Yu-Ping Tang, Qian-Ping Shi, Ze-Xi Dong, Peng-Xuan Zhang, Jin-Ao Duan; Investigation on the interactions of scutellarin and scutellarein with bovine serum albumin using spectroscopic and molecular docking techniques; Volume 38, Issue 10, October 2015, pages 1789-1801.

[8] Xiaodi Niu, Xiaohan Gao, Hongsu Wang, Xin Wang, Song Wang; Insight into the dynamic interaction between different flavonoids and bovine serum albumin using molecular dynamics simulations and free energy calculations; Volume 19, Issue 3, March 2013, pages 1039-1047.

[9] Hai Wu, Xiaojuan Zhao, Po Wang[a], Zong Dai, Xiaoyong Zou; Electrochemical site marke r competitive method for probing the binding site and binding mode between bovine serum albumin and alizarin red S; Volume 56, Issue 11, 15 April 2011, Pages 4181–4187.

[10] Ebrahim Balali; Thermodynamic Investigation of Tripeptide Tyr-Aaa-Gly in Gas Phase in Different Solvent; Oriental Journal of Chemistry,**Volume 30, 2014, pages** 623-629.

[11] Ammar A. Ibrahim and Rosiyah Yahya; Solvent Effects on N-Phthaloyl Chitosan Polymer: Prediction of Solubility in Different Solvents Using Theoretical Calculations; Asian Journal of Chemistry; Volume 23, No. 7 ,2011, pages 2956-2960.

[12] M. Kandasamy, G. Velraj, S. Kalaichelvan; Vibrational spectra, NMR and HOMO–LUMO analysis of 9-fluorenone-2-carboxylic acid; Spectrochimica Acta Part A: Molecular and Biomolecular Spectroscopy 105, 2013, pages 176–183.

[13] A. Suvitha, S. Periandy, M. Govindarajan, P. Gayathri; Vibrational analysis using FT-IR, FT-Raman spectra and HF–DFT methods and NBO, NLO, NMR, HOMO–LUMO, UV and electronic transitions studies on 2,2,4-trimethyl pentane; Spectrochimica Acta Part A: Molecular and Biomolecular Spectroscopy 138 , 2015, pages 900–912.

METHODOLOGY

CHAPTER 3
METHODOLOGY

3.1 INTRODUCTION

Chemistry is a science deals with construction, transformation and properties of molecules. Theoretical chemistry is the subfield, where mathematical methods are combined with fundamental laws of physics to study processes of chemical relevance [1]. Computational chemistry is focused on obtaining results relevant to chemical problems, not directly at developing new theoretical methods. There is a strong interplay between traditional theoretical chemistry and computational chemistry. The term theoretical chemistry is defined as a mathematical description of chemistry, whereas computational chemistry is used, when a mathematical method is sufficiently developed and automated for implementation on a computer. In theoretical chemistry, chemists, physicists and mathematicians develop algorithms, computer programs to predict atomic, molecular properties and reaction paths for chemical reactions. Computational chemistry applies the existing computer programs and methodologies to specific chemical questions.

3.2 DOCKING

Molecular docking is a computational problem, which predicts the preferred orientation of one molecule to a second when bound to each other to form a stable complex [2]. Molecular docking is one of the most frequently used methods in structure-based drug design. Due to its ability it predicts the binding-conformation of small molecule ligands to the appropriate target binding site. Characterisation of the binding behaviour plays an important role in rational design of drugs and to find out the fundamental biochemical processes [3]. The docking problem can predict their correct bound association for the given atomic coordinates of two molecules [4], which is the relative orientation and position after interaction. In the molecular docking problem, the two molecules are named as receptor and ligand. Usually, the smaller molecule is chosen as the ligand. There are two variation of molecular docking. The simpler problem is bound docking. It attempts to reconstruct a complex using the bound structures of the receptor and the ligand [5][6][7]. A bound structure is extracted from a structure containing more than one molecule, typically a complex of the receptor and the ligand. The more difficult problem is predictive docking, also referred to as the unbound docking [8]. It attempts to reconstruct a complex using the unbound structures of the receptor and the ligand. A protein in its unbound structure usually

undertakes conformation changes to bind with the other molecule, the 3D shapes of the protein changes. An unbound structure may be a native structure or a pseudo-native structure. A native structure is the structure of a molecule, when it is free in solution. A pseudo-native structure is the structure of a molecule when complexed with a molecule different from the one used in the docking problem.

3.2.1 MAJOR STEPS IN MOLECULAR DOCKING

STEP I – BUILDING THE RECEPTOR

In this step the 3D structure of the receptor is downloaded from PDB; later the available structure should be processed. This should include removal of the water molecules from the cavity, stabilizing the charges, filling the missing residues, generation the side chains etc according to the parameters available. The receptor should be biological active and stable state.

STEP II – IDENTIFICATION OF THE ACTIVE SITE

After the receptor preparation, the active site within the receptor should be identified. The receptor may have many active sites but the one of the interest should be selected. Most of the water molecules and heteroatom if present should be removed.

STEP III – LIGAND PREPARATION

Ligands can be obtained from various databases like PubChem or can be sketched using Chemsketch. Ligands were subjected to automatic preparation process, performed with LigPrep tool of the Schrodinger package [9]. It generates all possible protonation and tautomeric states available within a pH range of 7.0 ± 2.0.

STEP IV- DOCKING

This is the last step, where the ligand is docked onto the receptor and the interactions are checked. The scoring function generates score depending on which the best fit ligand is selected.

3.3 COMPUTATIONAL CHEMISTRY

Computational chemistry is a branch of chemistry that uses computer simulation in solving chemical problems. Computational chemistry have become a useful way to investigate materials that are too difficult to find or too expensive to purchase. Computational chemistry also helps chemists make predictions before carrying out the actual experiments so that they can make better observations. Scientist use Schroedinger equation as the basis for most of the computational chemistry calculations. This is because the Schroedinger equation models the atoms and molecules with mathematics. All molecular modeling techniques can

be classified under three major categories: ab initio electronic structure calculations, semi-empirical methods and molecular mechanics. General characteristics for each method are summarized below.

3.3.1 AB INITIO METHODS

Over the past three decades, ab initio quantum chemistry has become an essential tool in the study of atoms and molecules and also in modeling complex systems in biology and materials science. The term ab initio was first used in quantum chemistry by Robert Parr and co-workers, including David Craig in a semi-empirical study on the excited states of benzene [10][11]. The underlying core technology is computational solution of the electronic Schrodinger equation; given the positions of a collection of atomic nuclei, and the total number of electrons in the system, calculate the electronic energy, electron density, and other properties by means of a well defined, automated approximation. The ability to obtain good solutions to the electronic Schrodinger equation for systems containing tens, or even hundreds, of atoms has revolutionized the ability of theoretical chemistry to address important problems in a wide range of disciplines. For small molecules in the gas phase and in solution, ab initio quantum chemical calculations can provide results approaching benchmark accuracy [12], and they are used routinely to complement experimental studies. A wide variety of properties, including structures [13], thermo-chemistry, spectroscopic quantities of various types, and responses to external perturbations, can be computed effectively.

3.3.2 DENSITY FUNCTIONAL THEORY (DFT)

Density function theory (DFT) is an approach to the electronic structure of atoms and molecules which has enjoyed a dramatic surge of interest since the late 1980s. It is a computational quantum mechanical modelling method used in physics, chemistry and materials science. Using this theory, the properties of a many-electron system can be determined by using functionals, which in this case is the spatially dependent electron density. Hence the name density functional theory comes from the use of functionals of the electron density . DFT is among the most popular and versatile methods available in condensed-matter physics, computational physics, and computational chemistry. However, the real break- through came with a paper by Hohenberg and Kohn in 1964, showed that ground-state energy and other properties of a system were unique defined by the electron density. This is sometimes expressed by starting that the energy E, is a unique functional of

$\rho(r)$. A functional enables a function to be mapped to a number and is usually written using square brackets.

$$Q[f(r)] = \int f(r)dr \qquad (1)$$

The function $f(r)$ is usually dependent upon other well-defined functions. In the case of DFT the function depends upon the electron density, which would make Q a functional of $\rho(r)$; in the simplest case $f(r)$ would be equivalent to the density. In DFT the energy functional is written as a sum of two terms:

$$\mathrm{E}[\rho(r)] = \int V_{ext}(r)\,\rho(r)dr + F[\rho(r)] \qquad (2)$$

The first term arises from the interaction of the electrons with an external potential $V_{ext}(r)$. $F[\rho(r)]$ is the sum of the kinetic energy of the electron and the contribution from inter-electronic interactions. The minimum value is the energy corresponds to the exact ground-state electron density. There is a constraint on the electron density as the number of electrons (N) is fixed:

$$\mathrm{N} = \int \rho(r)dr \qquad (3)$$

In order to minimise the energy Lagrangian multiplier (-μ) is introduced leading to:

$$\frac{\delta}{\delta\rho(r)}\left[\mathrm{E}[\rho(r)] - \mu\int \rho(r)dr\right] = 0 \qquad (4)$$

From this we can write:

$$\left(\frac{\delta E[\rho(r)]}{\delta\rho(r)}\right)_{V_{ext}} = \mu \qquad (5)$$

This is the DFT equivalent of the Schrodinger equation. The subscript V_{ext} indicates that this is under conditions of constant external potential. The second landmark paper in the development of DFT was by Kohn and Sham who suggested a practical way to solve the Hohn berg-Kohn theorem for a set of interacting electron. From equation (2) it is not possible to know what function $F[\rho(r)]$ is. Kohn and Sham suggested that $F[\rho(r)]$ should be approximated as the sum of three terms.

$$F[\rho(r)] = E_{KE}[\rho(r)] + E_H[\rho(r)] + E_{XC}[\rho(r)] \quad (6)$$

Where $E_{KE}[\rho(r)]$ is the kinetic energy, $E_H[\rho(r)]$ electron-electron coulombic energy and $E_{XC}[\rho(r)]$ contains contributions from exchange and correlation. It is important to note that the first term $E_{KE}[\rho(r)]$ is defined as the kinetic energy of a system of non-interacting electrons with the same density $[\rho(r)]$ as the real system.

$$E_{KE}[\rho(r)] = \sum_{i=1}^{N} \int \psi_i(r) \left(-\frac{\nabla^2}{2}\right) \psi_i(r) dr \qquad (7)$$

The second term $E_H[\rho(r)]$ is also known as the Hartree electrostatic energy. In the Hartree approach, the electrostatic energy arises from the classical interaction between two charge densities which, when summed over all possible pair wise interactions gives:

$$E_H[\rho(r)] = \frac{1}{2} \iint \frac{\rho(r_1)\rho(r_2)}{|r_1 - r_2|} dr_1 dr_2 \qquad (8)$$

Combining these two and adding the electron-nuclear interaction leads to the full expression for the energy of an N-electron system within the Kohn and Sham scheme:

$$E_H[\rho(r)] = \sum_{i=1}^{N} \int \psi_i(r) \left(-\frac{\nabla^2}{2}\right) \psi_i(r) dr + \frac{1}{2} \iint \frac{\rho(r_1)\rho(r_2)}{|r_1 - r_2|} dr_1 dr_2$$
$$+ - \sum_{A=1}^{M} \int \frac{Z_A}{|r - R_A|} \rho(r) dr \qquad (9)$$

This equation acts to define the exchange correlation energy functional $E_{XC}[\rho(r)]$, which thus contains not only contributions due to exchange and correlation but also a contribution due to the difference between the true kinetic energy of the system and $E_{KE}[\rho(r)]$.

Kohn and Sham wrote the density $\rho(r)$ of the system as the sum of the square module of a set of one-electron orthonormal orbitals:

$$\rho(r) = \sum_{i=1}^{N} |\psi_i(r)|^2 \qquad (10)$$

By introducing this expression for the electron density and applying the appropriate variational condition the following one-electron Kohn and Sham equation results:

$$\left\{-\frac{\nabla_1^2}{2} - \left(\sum_{A=1}^{M} \frac{Z_A}{r_{1A}}\right) + \int \frac{\rho(r_1)}{r_{12}} dr_2 + V_{XC}[r_1]\right\} \psi_i(r) = \epsilon_i \psi_i(r_1) \qquad (11)$$

A self consistent approach is taken to solve the Kohn-Sham equation. An initial guess of the density is fed into equation (11) from which a set of orbitals can be derived, leading to an improved value for the density, which is then used in the second iteration and so on until convergence is achieved [14].

3.3.3 MOLECULAR MECHANICS

Molecular mechanics (MM) is often the only feasible means, which is used to model very large and non-symmetric chemical systems such as proteins or polymers. Molecular mechanics is a purely empirical method that neglects explicit treatment of electrons. As a result, MM calculations cannot deal with problems such as bond breaking or formation, where electronic or quantum effects dominate. Furthermore, MM models are system-dependent. MM energy predictions tend to be meaningless as absolute quantities, and are generally useful only for comparative studies. Despite these shortcomings, MM bridges the gap between quantum and continuum mechanics, and has been used quite extensively to study 'mesoscopic' effects in energetic materials. Applications include modelling reaction and dissociation on classical potential energy surfaces [15-18], studies of equilibrium crystal properties *(e.g.*, density, packing, specific heats) [19-23], dynamic investigations of shock interactions with crystals and defects [24], and simulating detonation in molecular crystals [25-28]. The basic assumptions of typical molecular mechanics methods are listed below:

• Each atom (i.e., electrons and nucleus) is represented as one particle with a characteristic mass.

• A chemical bond is represented as a spring with a characteristic force constant determined by the potential energy of interaction between the two participating atoms. Potential energy functions can describe intramolecular bond stretching, bending and torsion, or infer-molecular phenomena such as electrostatic interactions or van der Waals forces.

• The potential energy functions really on empirically derived parameters obtained from experiments or from other calculations.

3.3.4 SEMI-EMPIRICAL MODELS

Most molecular computations done by organic chemists those having minimum energy geometries, are done using this model because it provides the best compromise between speed and accuracy. This model is a hybrid of molecular mechanics-type models based on experimentally measured empirical data and pure theory quantum chemical or ab intio models, thus the name semi-empirical. It uses the Schrödinger equation approximations, make the calculations less time-consuming, it only calculates the locations of valence

electrons, not all electrons. For the inner shell electrons, empirical data from typical organic molecules is used to estimate their locations. Semi-empirical method is used for molecules containing 100 or more non-hydrogen atoms, much larger than those that can be modelled by the more rigorous ab initio models. However, Semi-empirical methods have been calibrated to typical organic or biological systems and tend to be inaccurate for problems involving hydrogen-bonding, chemical transitions or nitrated compounds [29-32]. Some of the more common semi-empirical methods can be grouped according to their treatment of electron-electron interactions [33].

3.4 BASIS SETS

The basis set is the set of mathematical functions from which the wave function is constructed. Each molecular orbital in HF theory is expressed as a linear combination of basis functions, the coefficients for which are determined from the iterative solution of the HF SCF equations that describe the shape of atomic orbitals. The full HF wave function is expressed as a Slater determinant formed from the individual occupied molecular orbitals. The HF limit is achieved by use of an infinite basis set, which necessarily permits an optimal description of the electron probability density. If the finite basis is expanded towards an infinite complete set of functions, calculations using such a basis set are said to approach the basis set limit. Keeping the total number of basis functions to a minimum is computationally attractive. Thus, a larger basis set can represent a computational improvement over a smaller basis set if evaluation of the greater number of integrals for the former can be carried out faster than for the latter. The basis functions must be chosen to have a form that is useful in a chemical sense. That is, the functions should have large amplitude in regions of space where the electron probability density is also large, and small amplitudes where the probability density is small [34].

3.4.1 CLASSIFICATION OF BASIS SET

(a) MINIMUM BASIS SET

A minimal basis set contains just the number of functions that are required to accommodate all the filled orbitals in each atom. In practise a minimal basis set normally includes all of the atomic orbitals in the shell. The basis sets STO-3G, STO-4G etc are all minimal basis sets.

(b) DOUBLE ZETA

A basis set which doubles the number of functions in the minimal basis set is described as a double Zeta basis set. The term zeta stems from the fact that the exponent of STO basis functions is often denoted by the Greek letter z.

(c) SPLIT VALENCE BASIS SETS

In split valence basis sets, additional basis functions are allocated to each valence atomic orbital. The resultant linear combination allows the atomic orbitals to adjust independently for a given molecular environment. Examples of split-valence sets are 3-21G, 4-31G, and 6-311G etc [35].

(d) POLARISED BASIS SETS

Polarization functions can be added to basis sets to allow for non-uniform displacement of charge away from atomic nuclei, thereby improving descriptions of chemical bonding. The use of polarization basis function is indicated by an asterisk (*). Thus 6-31G* refers to a 6-31G basis set with polarization functions on the heavy atoms.

(e) DIFFUSE BASIS SETS

The diffuse functions can be added to the basis set. These basis set are denoted using a '+', thus the 3-21+G basis set contains an additional single set of diffuse s-type and p-type Gaussian functions. '++' indicated that the diffuse functions are included for hydrogen as well as for heavy atoms.

(f) HIGH ANGULAR MOMENTUM BASIS SETS

High angular momentum basis sets augmented with diffuse functions represent the most sophisticated basis sets available. Examples of high angular momentum basis sets are 6-31G (2d), 6-311G (2df, pd), and 6-311G (3df, 2df, p)., and the time allotted for the studies.

3.5 GEOMETRICAL PARAMETERS

3.5.1 BOND LENGTH

Distances between centers of bonded atoms are called bond lengths, or bond distances. Bond lengths vary depending on many factors, but in general, they are very consistent. Of course the bond orders affect bond length, but bond lengths of the same order for the same pair of atoms in various molecules are very consistent. The length of the bond is determined by the number of bonded electrons (the bond order). The higher the bond order, the stronger will be the attraction between the two atoms and the shorter the bond length. Generally, the length of the bond between two atoms is approximately the sum of the covalent radii of the two atoms.

Bond length is reported in picometers. Therefore, bond length increases in the given order: triple bond < double bond < single bond. Bond lengths are determined by X-ray diffraction of solids, by electron diffraction, and by spectroscopic methods. The bond length between two atoms is shown in fig: 3.1.

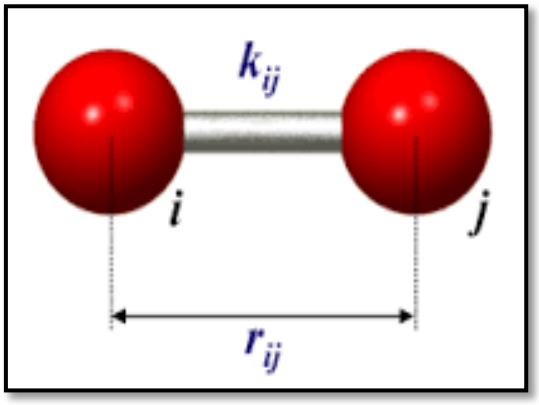

Fig: 3.1 Bond Length

3.5.2 BOND ANGLE

The angles between the lines representing the two bonds are known as bond angles and are measured by X-ray diffraction and spectroscopic methods. Because of the constant atomic vibrations, the bond angles thus measured are really average bond angles. The shapes of the molecules are dependent on the bond angles. The molecule of methane, therefore, is tetrahedral because of the H—C—H bond angles of 109.5°. The bond angle for methane molecule is shown in fig: 3.2.

Fig: 3.2 Bond Angle

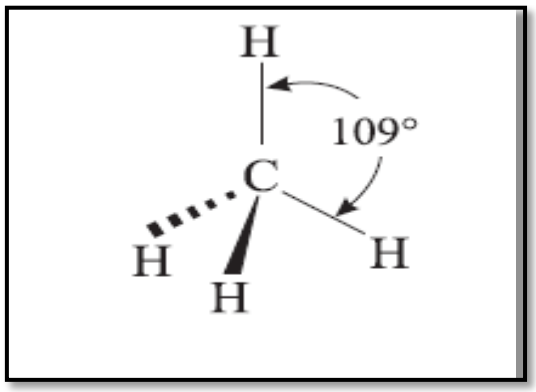

3.6 UV-VIS SPECTRUM

UV-VIS spectrum results from the interaction of electromagnetic radiation in the UV-VIS region with molecules, ions, or complexes. The absorption of radiation in the UV-VIS region of the spectrum is dependent on the electronic structure of the absorbing species like, atoms, molecules, ions or complexes. A given electronic energy level has a number of vibrational energy levels in it and each of the vibrational energy level has a number of rotational energy levels in it. When a photon of a given wavelength interacts with the molecule it may cause a transition amongst the electronic energy levels if its energy matches with the difference in the energies of these levels. UV-VIS spectroscopy is also known as electronic spectroscopy in which, the amount of light absorbed at each wavelength of UV and visible regions of electromagnetic spectrum is measured. As a result of absorption of electromagnetic radiation molecular transitions occur. These transitions occur between the electronic energy levels. As a molecule absorbs energy, an electron is promoted from occupied orbital to an unoccupied orbital of greater potential energy. Generally the most probable transition is from HOMO to LUMO.

3.7 NUCLEAR MAGNETIC RESONANCE SPECTROSCOPY (NMR)

Nuclear magnetic resonance spectroscopy (NMR) was first developed in 1946. NMR spectroscopy is a research technique that exploits the magnetic properties of certain atomic nuclei. It determines the physical and chemical properties of atoms or the molecules in which they are contained. It relies on the phenomenon of nuclear magnetic resonance and can provide detailed information about the structure, dynamics, reaction state, and chemical environment of molecules. The intramolecular magnetic field around an atom in a molecule changes the resonance frequency, thus giving access to details of the electronic structure of a molecule. Most frequently, NMR spectroscopy is used to investigate the properties of organic molecules, although it is applicable to any kind of sample that contains nuclei possessing spin. Suitable samples range from small compounds analyzed with 1-dimensional proton or carbon-13 NMR spectroscopy to large proteins or nucleic acids using 3 or 4-dimensional techniques. The impact of NMR spectroscopy on the sciences has been substantial because of the range of information and the diversity of samples, including solutions and solids. NMR spectra are unique, well-resolved, analytically tractable and often highly predictable for small molecules. Thus, in organic chemistry practice, NMR analysis is used to confirm the identity of a substance.

3.8 INFRARED SPECTROSCOPY

Infrared spectroscopy or Vibrational Spectroscopy deals with the infrared region of the electromagnetic spectrum, that is light with a longer wavelength and lower frequency than visible light. It covers a range of techniques, mostly based on absorption spectroscopy. As with all spectroscopic techniques, it can be used to identify and study chemicals. For a given sample which may be solid, liquid, or gaseous, the method or technique of infrared spectroscopy uses an instrument called an infrared spectrometer (or spectrophotometer) to produce an infrared spectrum. A basic IR spectrum is essentially a graph of infrared light absorbance (or transmittance) on the vertical axis vs. frequency or wavelength on the horizontal axis. Typical units of frequency used in IR spectra are reciprocal centimeters (sometimes called wave numbers). A common laboratory instrument that uses this technique is a Fourier transform infrared (FTIR) spectrometer. The infrared portion of the electromagnetic spectrum is usually divided into three regions; the near-, mid- and far-infrared, named for their relation to the visible spectrum. The higher-energy near-IR, approximately 14000–4000 cm^{-1} can excite overtone or harmonic vibrations. The mid-infrared, approximately 4000–400 cm^{-1} may be used to study the fundamental vibrations and associated rotational-vibrational structure. The far-infrared, approximately 400–10 cm^{-1} lying adjacent to the microwave region, has low energy and may be used for rotational spectroscopy. The names and classifications of these sub-regions are conventions, and are only loosely based on the relative molecular or electromagnetic properties.

3.9 COMPUTATIONAL DETAILS OF THE PRESENT STUDY

- The structure of Alizarin is optimized by using DFT method with B3LYP using DFT method with B3LYP level using 6-311++G (d,p) basis set.
- Using the optimized structure, geometrical parameters like Bond length, Bond angle and Dihedral angle of Alizarin is determined by using the same level of theory.
- Vibrational assignments (IR and Raman) of Alizarin have been computed by the same level of theory.
- Absorption spectrum for Alizarin and Alizarin with different solvents have been calculated bt TD-DFT method.
- NMR spectrums have been analyzed by using GIAO method.

3.10 REFERENCES:

[1] T.Schlick, Molecular Modeling and Simulation, Springer,2002.

[2] Lengauer T, Rarey M (Jun 1996). "Computational methods for biomolecular docking". Current Opinion in Structural Biology 6 (3): 402–6.

[3] Kitchen DB, Decornez H, Furr JR, Bajorath J (Nov 2004). "Docking and scoring in virtual screening for drug discovery: methods and applications". Nature Reviews. Drug Discovery 3 (11): 935–49.

[4] Halperin I, Ma B, Wolfson H, and Nussinov R; Principles of docking: An overview of search algorithms and a guide to scoring functions. PROTEINS: Structure, Function, and Genetics, 2002, 47:409-443.

[5] Goldman BB, Wipke WT (2000). "QSD quadratic shape descriptors. 2. Molecular docking using quadratic shape descriptors (QSDock)". Proteins **38** (1): 79–94.

[6] Meng EC, Shoichet BK, Kuntz ID (2004). "Automated docking with grid-based energy evaluation". Journal of Computational Chemistry **13** (4): 505–524.

[7] Morris GM, Goodsell DS, Halliday RS, Huey R, Hart WE, Belew RK, Olson AJ (1998). "Automated docking using a Lamarckian genetic algorithm and an empirical binding free energy function". Journal of Computational Chemistry **19** (14): 1639–1662.

[8] Feig M, Onufriev A, Lee MS, Im W, Case DA, Brooks CL (Jan 2004). "Performance comparison of generalized born and Poisson methods in the calculation of electrostatic solvation energies for protein structures". Journal of Computational Chemistry **25** (2): 265–84.

[9] LigPrep, version 3.2, Schrödinger, LLC, New York, NY, 2014.

[10] Parr, Robert G. "History of Quantum Chemistry".

[11] Parr, Robert G.; Craig D. P.; Ross, I. G (1950). "Molecular Orbital Calculations of the Lower Excited Electronic Levels of Benzene, Configuration Interaction included". Journal of Chemical Physics 18 (12): 1561–1563.

[12] Martin, J. M. L. & de Oliveira, G. (1999) J. Chem. Phys. 111, 1843–1856.

[13] Thomas, J. R., Deeleeuw, B. J. Vacek, G., Crawford, T. D., Yamaguchi, Y. & Schaefer, H. F. (1993) J. Chem. Phys. 99, 403–416.

[14] A.R.Leach, molecular modelling principles and applications, Second edition 2001, Glaxo Wellcome Research and Development. Page no: 126-129.

[15] Sewell, T.D., and Thompson, D.L., (1991) Classical dynamics study of the unimolecular dissociation of Hexahydro-l,3-trinitro-l,3,5-triazine, Journal of Physical Chemistry 95, 6228-6242.

[16] Wallis, E.P., and Thompson, D.L. (1993) Molecular dynamics simulations of ring inversion in RDX, Journal of Chemical Physics 99 (4) 2661-2673.

[17] Rice, B.M., Grosh, J., and Thompson, D.L. (1995) Vibrational mode selectivity in the unimolecular decomposition of GHfeNNO^ Journal of Chemical Physics 102 (22) 8790-8799.

[18] Kohno, Y., Ueda, K., and Imamura, A. (1996) Molecular dynamics simulations of initial decomposition processes on the unique N-N bond in nitramines in the crystalline state, Journal of Physical Chemistry 100**,**4701-4712.

[19] Sorescu, D.C., and Thompson, D.L. (1997) Crystal packing and molecular dynamics studies of the 5-Nitro-2,4-dihydro-3H-l,2,4-triazol-3-one crystal, Journal of Physical Chemistry B101,3605-13.

[20] Sewell, T.D, Brill, T.B, T.P, Tao, W.C., and Wardle, R.B., Eds., Materials Research Society, Pittsburgh, PA, 67-72.

[21] Kunz, A.B., Brill, T.B., Russell, T.P, Tao, W.C., and Wardle, R.B., Eds., Materials Research Society, Pittsburgh, PA, (1996), 287-292.

[22] Dzyabchenko, A.V., Pivina, T.S., and Arnautova, E.A. (1996) Prediction of structure and density for organic nitiamines, Journal of Molecular Structure 378, 67-82.

[23] Filippini, G., and Gavezzotti, A., (1994) The crystal structure of 1,3,5-Triamino-2,4,6-trinitrobenzene. Centrosymmetric or non-centrosymmetric? Chemical Physics Letters 231, 86-92.

[24] Phillips, L., Sinkovits, R.S., Oran, E.S., and Boris, J.P., (1993) The interaction of shocks and defects in Lennard-Jones crystals, Journal ofPhysics, Condensed Matter 5, 6357-6376.

[25] Haskins, P.J., and Cook, M.D. (1998) Molecular dynamics studies of fast decomposition in energetic molecules, in Preprints of Proceedings of the 11th Symposium (International) on Detonation, Snowmass, CO, Office of the Chief of Naval Research, Arlington, VA, 104-108, and references therein.

[26] Eiert, M.L., Robertson, D.H., and White, C.T (1996) Molecular dynamics study of the effect of varying exothermicity on the properties of condensed-phase detonation, in Decomposition, Combustion and Detonation Chemistry of Energetic Materials, Materials Research Society Symposium Proceedings 418 Boston, MA (November 1995); 309-312.

[27] Barrett, J.C. Barrett, Robertson, D.H., Brenner, D.W., and White, C.T. (1996), Brill, T.B., RusseU, T.P, Tao, W.C, and Wardle, R.B.,Eds., Materials Research Society, Pittsburgh, PA, 301-308.

[28] Soulard, L, **Brill, T.B., RusseU, T.P, Tao, W.C, and Wardle, R.B., Eds.**, Materials Research Society, Pittsburgh, PA, (1996), 293-300.

[29] Akutsu, Y. and Tahara, S.Y. (1991) Calculations of heats of formation for nitro compounds by semi-empirical MO methods and molecular mechanics, Journal of Energetic Materials 9161-172.

[30] De Paz, J.L. and Ciller, J. (1993) On the use of AMI and PM3 methods on energetic compounds, Propellants, Explosives, Pyrotechnics 18,33-40.

[31] I.N. Levine, Quantum Chemistry, Boston: Allyn and Bacon, Inc. (1983).

[32] D.B. Cook, Handbook of Computational Quantum Chemistry, New York: Oxford University Press (1998).

[33] HyperChem 5.0 user manuals, Hypercube, Inc., FL (1996).

[34] Introduction to Computational Chemistry**,** Second Edition, Frank Jensen, (2007).

[35] A.R.Leach, molecular modelling principles and applications, Second edition 2001, Glaxo Wellcome Research and Development. Page no: 65-72.

RESULTS AND DISCUSSION

CHAPTER IV

RESULTS AND DISCUSSION

4.1 INTRODUCTION:

Anthraquinones are a family of organic compounds widely used for their pharmaceutical properties. Alizarin (AZ) is a naturally occurring Hydroxyanthraquinone. Hydroxyanthraquinones have attracted the attention of many researchers owing to their possible applications related to the photo activity based on their chromatic properties. Alizarin is the common name of 1,2-dihydroxyanthraquinone. This compound and its derivatives are used as colorimetric reagents in analytical chemistry. Like other anthraquinone dyes, it is a biologically active molecule and has remarkable antigenotoxic. The structural properties of the ground state and electronic absorption spectra of alizarin [1] and alizarin with solvents have been investigated [2] experimentally. Some organic dyes have been used as fluorescent probes of biological macromolecules and the photosensitizers therapy (PDT). PDT is mainly based on the selective accumulation of photosensitizer in diseased tissue and high photochemical reactivity.

In the present study an attempt has been made to theoretically interpret the molecular structure, fundamental vibrational frequencies and intensity of the vibrational bands of Alizarin by using structure optimizations in different solvents like Methanol (MeOH), DMSO, CCl_4. The calculations were done based on Density Functional Theory (DFT) method with B3LYP level using the basis set of 6-311++G (d,p). Absorption spectra for AZ and AZ with different solvents are also obtained by TD-DFT method by using Gaussian 09 software. The ^{1}H and ^{13}C nuclear magnetic resonance (NMR) chemical shifts of the molecule were also calculated by using the gauge independent atomic orbital method (GIAO).

Molecular docking is a fast and reliable tool for the study of inter-molecular interactions in the systems of biological and therapeutic significance. Bovine Serum Albumin (BSA) is the most abundant protein plasma contributing to osmotic blood pressure which plays important roles in the transport, distribution and metabolism of many exogenous ligand, including fatty acids, amino acids, drugs and pharmaceuticals. Being the major binding protein for drugs and other physiological substances, it is considered as a model protein for studying Drug-protein interaction in vitro. In the present study an attempt has been made to identify the nature of binding interactions of Alizarin (AZ) with Bovine Serum Albumin (BSA). The docking studies are done by using the maestro/Glide of Schrödinger software.

4.2 MOLECULAR GEOMETRY:

The structure of AZ and AZ with solvents like MeOH, DMSO, CCl_4 have been optimized by the theory of Density Functional theory with B3LYP/6-311++G (d,P) using Gaussian 09 and shown in fig: 4.1.

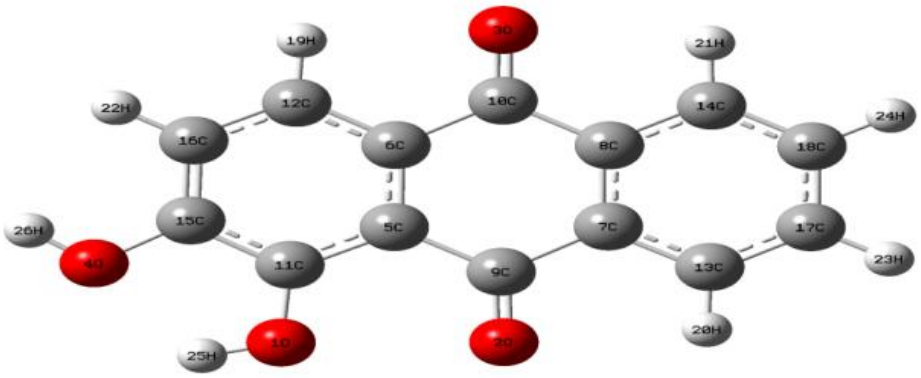

Fig: 4.1 optimized structure of AZ

From the optimized structure, the energy values are calculated for AZ and AZ in different solvents are tabulated and shown in table: 4.1.

TABLE: 4.1 Energy values of AZ and AZ in different solvents

Alizarin	-839.44277354 au
Alizarin + MeOH	-839.45031086
Alizarin + DMSO	-839.46053361
Alizarin + CCl_4	-839.46023778

From the optimized geometry, the geometrical parameters like Bond length, Bond angle and Dihedral angle of Alizarin were determined by using the same level of theory. Table 4.2, 4.3 and 4.4 shows the Bond length, Bond angle and Dihedral angle respectively.

TABLE 4.2: Bond length (Å) of AZ optimized by using DFT with B3LYP/6-311++G (d,P)

Parameters	**Bond length**
O1-O2	2.6615121
O2-O3	5.3990170
O1-O4	2.6177337
C2-C5	2.3820908
C5-C6	1.4187957
C2-C7	2.3569077
C7-C8	1.4030806
C2-C9	1.2180035
C3-C10	1.2221053
C1-C11	1.3478167
C6-C12	1.3916430
C7-C13	1.3988576
C8-C14	1.3993527
C4-C15	1.3708673
C15-C16	1.3844592
C13-C17	1.3893242
C14-C18	1.3886866
H12-H19	1.0818719
H13-H20	1.0827219
H14-H21	1.0828438
H16-H22	1.0857566
H17-H23	1.0841471
H18-H24	1.0840589
H1-H25	0.9678662
H4-H26	0.9626577

TABLE 4.3: Bond angle (deg) of AZ optimized by using DFT with B3LYP/6-311++G (d,P)

Parameters	**Bond angle**
O2-O1-O3	90.0748450
O1-O2-O4	148.2648110
C2-C1-C5	56.8151150
C5-C2-C6	145.8353875
C2-C1-C7	122.0645011
C7-C2-C8	148.6545439
C2-C1-C9	88.6128744
C3-C2-C10	0.2198524
C1-C5-C11	29.5496920
C6-C5-C12	120.8637018
C7-C2-C13	91.8195848
C8-C7-C14	119.9618020
C4-C1-C15	64.2913249
C15-C4-C16	124.2167305
C13-C7-C17	120.2216546
C14-C8-C18	120.1036529
H12-H6-H19	118.5618591
H13-H7-H20	118.3962059
H14-H8-H21	118.4396845
H16-H15-H22	119.9816222
H17-H13-H23	119.8505600
H18-H14-H24	119.9796866
H1-H11-H25	108.0202730
H4-H1-H26	175.3361479

TABLE 4.4: Dihedral angle (deg) of AZ optimized by using DFT with B3LYP/6-311++G (d,P)

Parameters	Dihedral angle
C5-C2-C1-C6	180.0000
C1-C5-C2-C11	180.0000
C6-C5-C2-C12	180.0000
C7-C2-C1-C13	180.0000
C8-C7-C2-C14	180.0000
C15-C4-C1-C16	180.0000
C13-C7-C2-C17	180.0000
H12-H6-H5-H19	180.0000
H14-H8-H7-H21	180.0000
H17-H13-H7-H23	180.0000
H18-H14-H8-H24	180.0000
H1-H11-H5-H25	180.0000

4.3 VIBRATIONAL ASSIGNMENTS

Spectroscopy involves the study of the interaction of electromagnetic radiation with matter [3]. The amount of energy absorbed by the molecule gives the information about the structure of the molecule [4]. The vibrational spectrum is mainly determined by the modes of free molecules observed at higher wave numbers, together with the lattice (translational and vibrational) modes in the low wave number region. Each dip in the spectra is called a band or peak and represents absorption of IR at that frequency by the sample [5].

Alizarin is a non-linear molecule and it has 3N-6 degrees of freedom. It consists of 26 atoms therefore they have 72 vibrational normal modes. The modes of vibrations are of two types. They are stretching and bending.

STRETCHING

In Stretching vibrations, the atoms move along the bond axis, so that the bond length increases or decreases at regular intervals. But the atoms remain in the same bond axis. There are two types of stretching.

(a) Symmetric stretching

In symmetric stretching two attached atoms move away and towards the central atom at the same time.

(b) Asymmetric stretching:

In asymmetric stretching two attached atoms do not move away and towards the central atom at the same time.

BENDING

Bending vibrations may consist of a change in bond angle between bonds with a common atom. There are four types of bending vibrations [6].

(a) Scissoring

Two atoms move away and towards each other is called scissoring.

(b) Rocking

It is like the motion of pendulum in which the atom is pendulum and there are two instead of one.

(c) Wagging

Two atoms swing back and forth out the plane of molecule.

(d) Twisting

Two atoms rotate about the bond which joins it to the remainder of the molecule.

The IR and Raman spectra are shown in the figure: 4.3 and 4.4. The strongest peak of IR vibration spectrum is at 1294.0207 cm^{-1}. But in Raman spectrum the strongest peak corresponds to 1714.8888 cm^{-1}. The second highest peak of IR spectrum is 1729.5459 cm^{-1}. The second highest peak of Raman spectrum is 3845.9775 cm^{-1}.

The frequency mode of vibration of alizarin optimized at DFT/6-311++G (d,p) level of theory are shown in the table: 4.5.

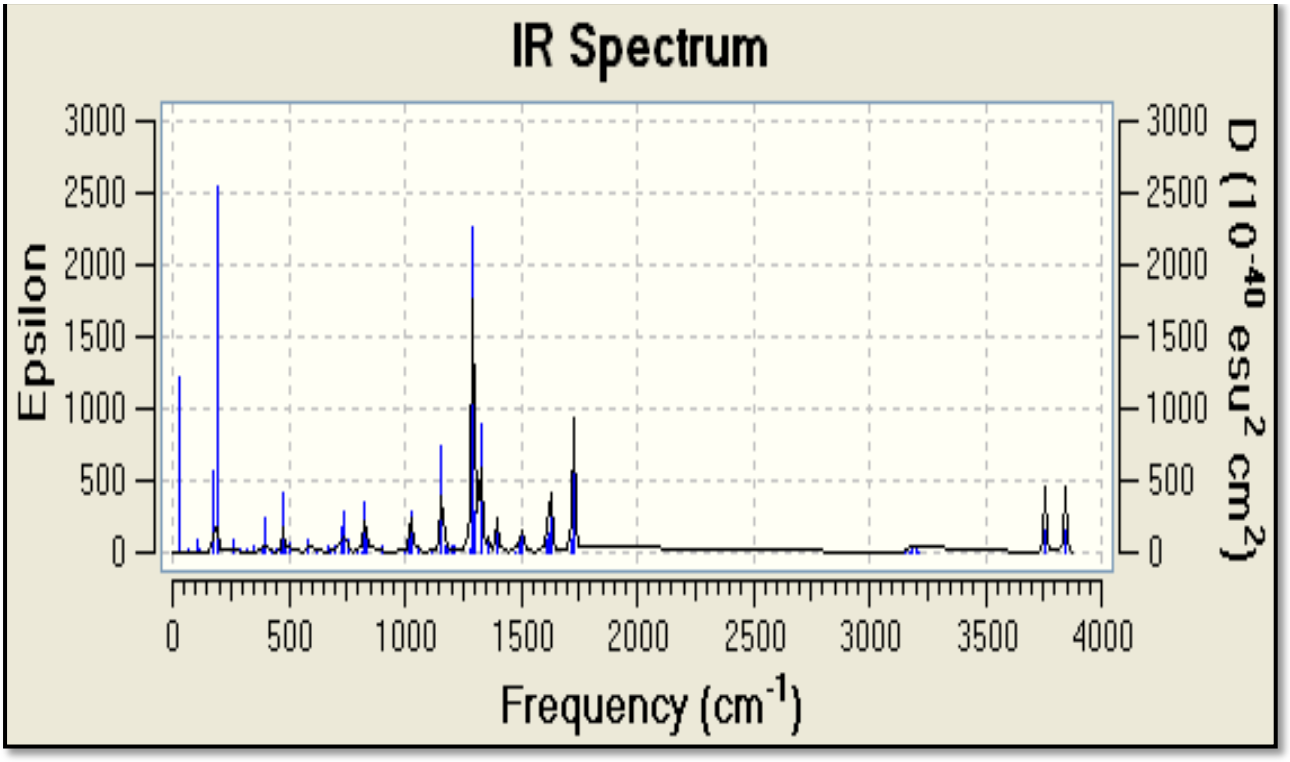

Fig: 4.2 A graph between frequency vs IR intensities of AZ

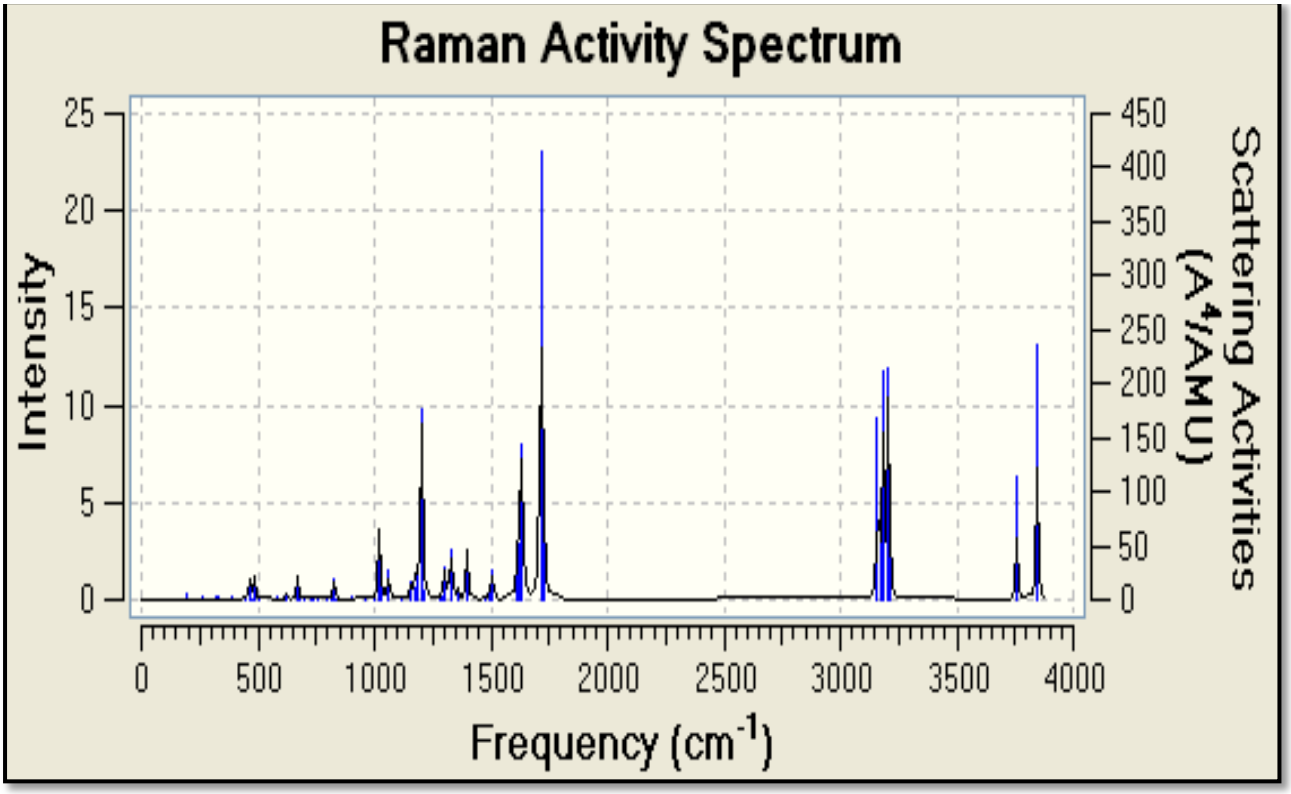

Fig: 4.3 A graph between frequency vs Raman intensities of AZ

4.3.1 RING VIBRATIONS

The ring stretching vibrations are very prominent in the ring. The C-C stretching modes are observed at 1017.0926, 1159.1149, 1180.4382, and 1278.3626 cm^{-1}. C-C-C in plane bending modes is observed at 1180.4382 cm^{-1}.

4.3.2 C=O VIBRATIONS

The carbon–oxygen double bond is formed by pp–pp bonding between carbon and oxygen internal hydrogen bonding. It reduces the frequencies of the C=O stretching absorption to a greater degree than does inter molecular H bonding because of the different electronegativity of C and O, the bonding are not equally distributed between two atoms. Normally carbonyl group vibrations occur in the region 1850-1600 cm^{-1} [7].

In our present investigation, the theoretical calculations predict the C=O stretching vibrational modes at 1729.5459, 1634.5111, 1629.0142 and 1619.5537 cm^{-1} by B3LYP/6-311++G (d,p) level.

4.3.3 C-H VIBRATIONS

The C-H in plane ring bending vibrations are normally occurs as a number of strong to weak intensity bands in the region 1300-1000 cm^{-1} [7]. In the present work, the C-H in plane bending vibrations of the Alizarin molecule is identified at 1159.1149 and 1180.4382 cm^{-1}.

The out of plane bending of the ring C-H bonds are normally found in the region 960-675 cm^{-1}. And these bands are highly informative [7]. The C-H out of plane bending vibrations are observed at 827.363 and 906.5263 cm^{-1}. The theoretical in plane and out of plane bending vibrational wave numbers are found to be well within their characteristic region.

4.3.4 OH VIBRATIONS

OH bending vibrations are observed at 1334.0202, 1396.6876, 1629.0142 cm^{-1} (scissoring).

TABLE 4.5 : Frequency mode of vibration of Alizarin optimized at DFT/6-311++G(d,p) level of theory

Sl.No.	DFT/ 6311++G (d,p)		Assignments
	Observed value (cm^{-1})	Standard value (cm^{-1})	
1	331.1218	339w	Skeletal vibration
2	393.884	396	Skeletal vibration
3	463.8803	464	υ_{sym} (ring)
4	476.0623	473	Skeletal vibration
5	623.4804	615	$\rho(OH)$
6	669.6908	654	υ(ring)
7	681.8728	679	$\rho(ring)$
8	827.363	826w	γ(C-H)/ γ(C-O)
9	906.5263	900w	γ(C-H)
10	1002.1692	1004	υ_{asym} (ring)
11	1017.0962	1013m	υ(CC)/δ(CCC)
12	1030.6571	1027	υ(H_{ring})
13	1159.1449	1157s	υ(CC)/δ(CH)
14	1180.4382	1186s	υ(CC)/ δ(CH)/δ(CCC)
15	1278.3626	1273	υ(ring)
16	1294.0207	1292	δ(H_{ring})
17	1334.0206	1335	δ(OH), υ(ring)
18	1396.6876	1389	δ(OH), υ(ring)
19	1619.5537	1623w,br	υ(C=O)
20	1629.0142	1629	υ(C=O), δ(OH), υ(ring)
21	1634.5111	1633m	υ(C=O)
22	1729.5459	1738vs	υ(C=O)

w- weak, m- medium, s- strong, vs- very strong, br- broad, $\upsilon -$ stretching, δ– in-plane bending, γ– out-of-plane bending, ω- wagging, ρ- rocking

4.4 UV–VIS SPECTRA ANALYSIS

The broad absorption bands associated to a strong $\pi \rightarrow \pi^*$ and a weak $\sigma \rightarrow \sigma^*$ transition characterize the UV–Vis absorption spectra. Natural bond orbital analysis indicates that molecular orbitals are mainly composed of σ and π atomic orbitals [8]. The electronic absorption spectra of the compound alizarin in methanol, DMSO and CCl_4 as solvents were recorded within the 200–600 nm range. Electronic absorption spectra were calculated using the TD-DFT method based on the B3LYP/6-311++G (d,p) level optimized structure in gas phase. TD-DFT calculations of the title compound in methanol, DMSO and CCl_4 as solvents were performed using the PCM model. The theoretically predicted UV spectra by TD-DFT level are shown in Fig: 4.2. The electronic absorption spectra showed two bands at 238.8 and 380.4 nm for vacuum, for methanol three bands are obtained at 207.6, 247.2 and 403.2 nm, for CCl_4 only one band is obtained at 397.6 nm and for DMSO the band is at 408.99.

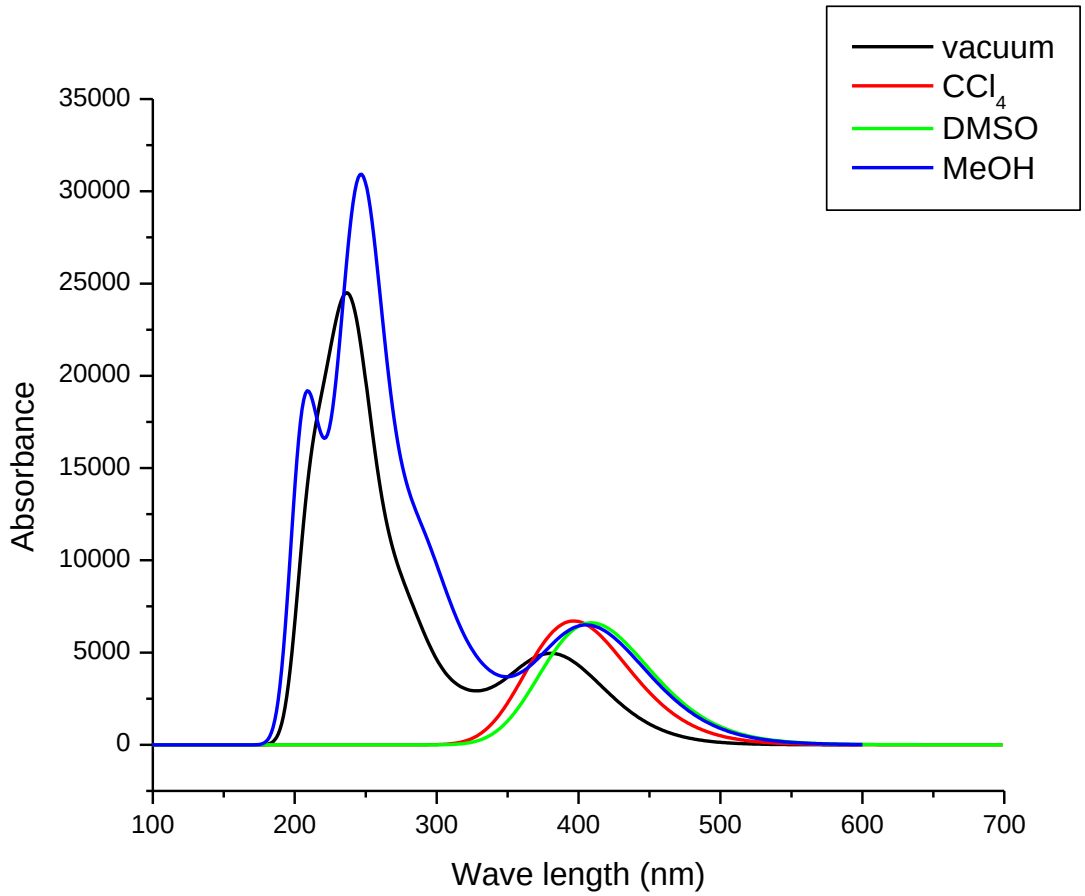

Fig: 4.4 UV spectum of AZ

4.5 NMR SPECTRA ANALYSIS

NMR spectroscopy has proved to be an exceptional tool to elucidate structure and molecular conformation. Firstly, full geometry optimization was performed at the gradient corrected density functional level of theory using the hybrid B3LYP method based on Becke's three parameters functional of DFT. In order to provide an unambiguous assignment and analysis ^{1}H and ^{13}C NMR spectra, theoretical calculations on chemical shift for Alizarin were done by Gauge Independent Atomic Orbital (GIAO) method is shown in fig: 4.6. Relative chemical shifts were estimated by using the corresponding TMS shielding calculated in advance at the same theoretical levels as references. The theoretical ^{1}H and ^{13}C NMR isotropic chemical shifts for Alizarin are shown in the Table: 4.3. The ^{13}C and ^{1}H chemical shifts are calculated by B3LYP/6-311++G(d) level of theory for Alizarin with MeOH, CCl_4 and DMSO as solvents are shown in fig: 4.6, 4.7 and 4.8 respectively.

TABLE 4.6: The theoretical ^{1}H and ^{13}C NMR isotropic chemical shifts (with respect to TMS, all values in ppm) for Alizarin

Atom	Vacuum	MeOH	CCl_4	DMSO
C10	-4.3154	-6.7803	-6.7720	-5.4382
C9	-3.3715	-7.2327	-7.2476	-4.9843
H20	23.3323	23.3772	23.3795	23.3480
H21	23.5014	23.5202	23.5222	23.5076
H19	23.8892	23.8667	23.8674	23.8857
H23	24.1395	23.8852	23.8824	24.0301
H24	24.1419	23.8746	23.8717	24.0284
H22	25.0622	24.6012	24.5951	24.8685
H25	25.8123	25.1881	25.1684	25.5331
H26	27.5796	26.2701	26.2429	27.0008
C15	29.1556	26.5438	26.5085	28.0545
C11	29.7866	29.4947	29.4779	29.6422
C7	42.7119	42.6975	42.6808	42.7022
C17	44.1927	42.3136	42.2873	43.3966
C8	44.2626	44.0824	44.0696	44.1705
C18	44.9264	42.6777	42.6423	44.0198
C6	47.9758	49.7130	49.7473	48.7337
C13	50.0276	50.2798	50.2942	50.1190
C14	51.7099	51.7050	51.7157	51.6955
C5	58.0217	58.9420	58.9684	58.4027

C12	58.3245	56.5818	56.5366	57.6416
C16	64.1172	60.6501	60.6076	62.7542

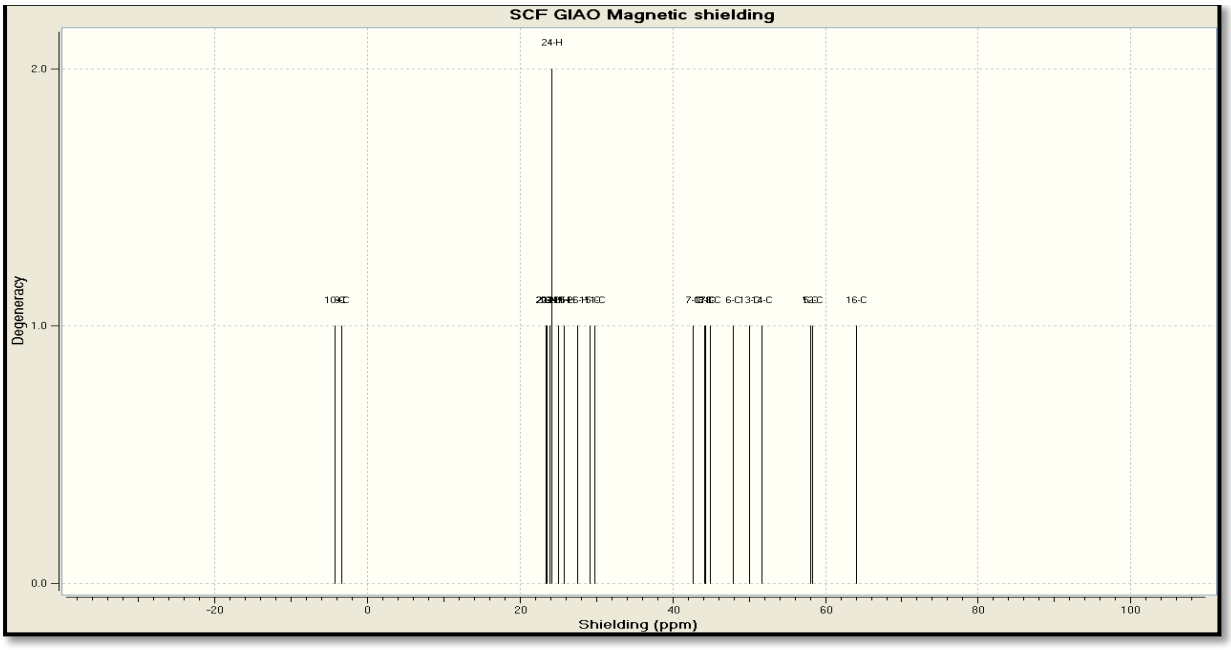

Fig: 4.5 The calculated ^{13}C and ^{1}H NMR isotropic chemical shifts (ppm) of Alizarin

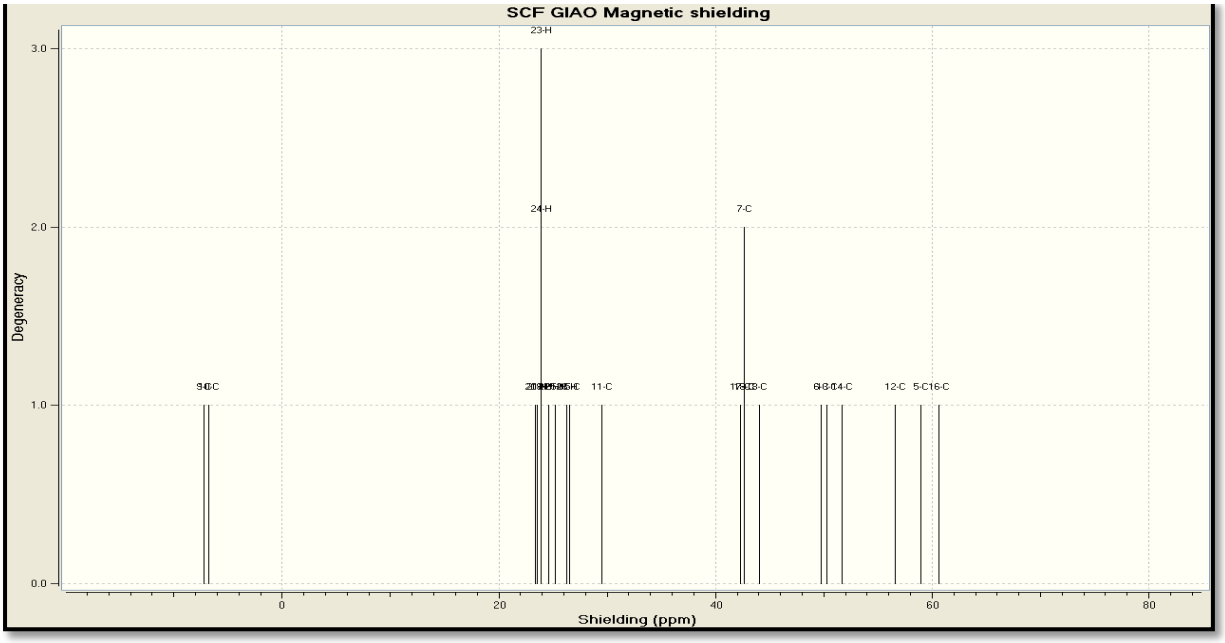

Fig: 4.6 The calculated ^{13}C and ^{1}H NMR isotropic chemical shifts (ppm) of AZ+MeOH

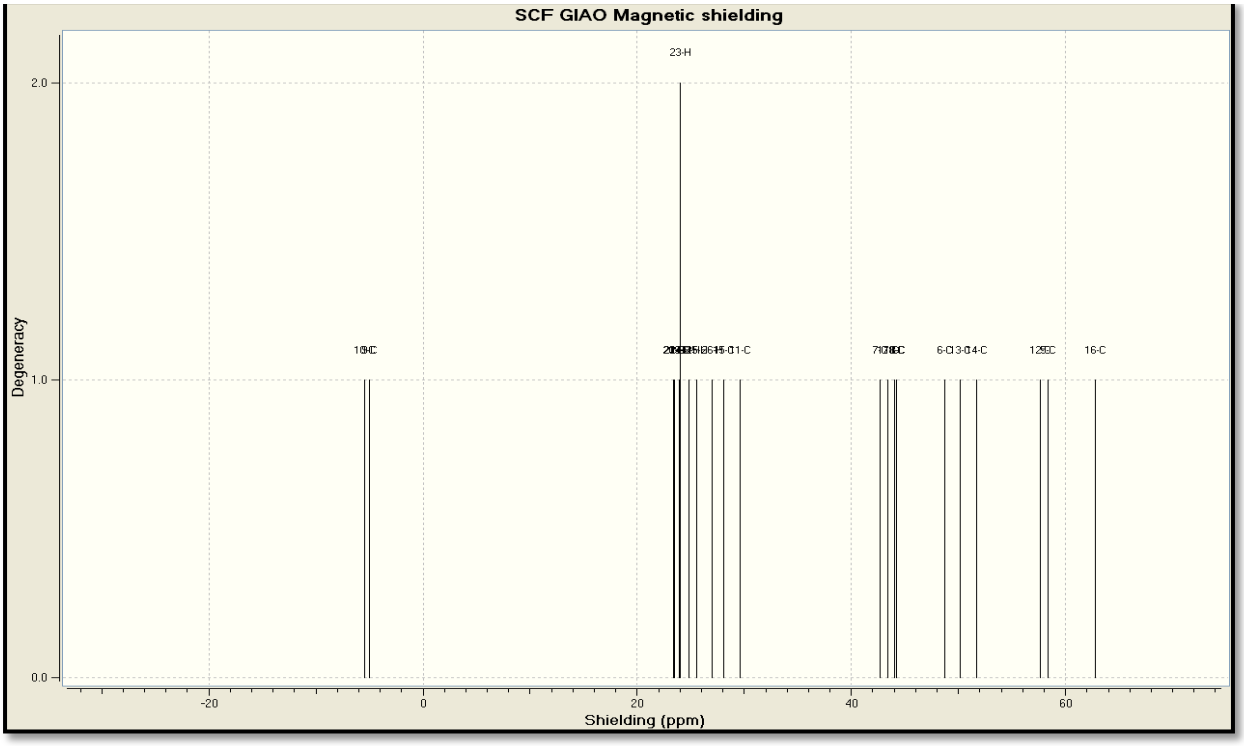

Fig: 4.7 The calculated ^{13}C and ^{1}H NMR isotropic chemical shifts (ppm) of AZ+CCl_4

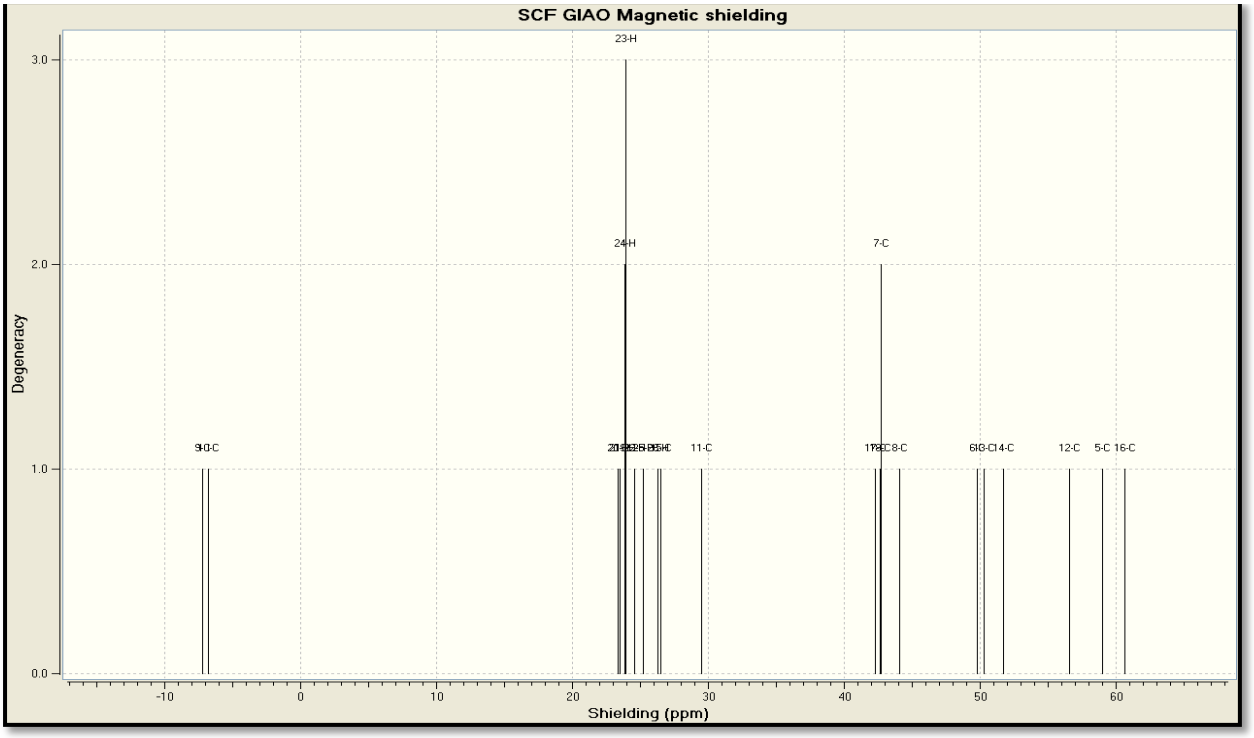

Fig: 4.8 The calculated ^{13}C and ^{1}H NMR isotropic chemical shifts (ppm) of AZ+DMSO

4.6 DOCKING STUDY

The amino acid sequence of Bovine Serum Albumin had been taken from NCBI database. PDB file of BSA is taken from PDB ID: 3VO3. Alizarin was docking with BSA protein molecule using the Glide in Maestro of Schrodinger software. Site Map, Schrödinger's program was used for identifying, evaluating, and visualizing ligand binding sites. A receptor grid was generated around the active site. The ligand-midpoint box was given a side of 10A°. The site score is 1.133. Ligands were subjected to automatic preparation process, performed with Lig Prep tool of the Schrodinger package. It generates all possible protonation and tautomeric states available within a pH range of 7.0±2.0. The prepared and optimized ligands were flexibly docked in the grid box of the protein. Glide Score (GScore) was used to rank the ligands on the basis of their relative binding affinities.

4.6.1 BINDING SITE AND BINDING MODE

The modeled and refined protein was docked against Alizarin. Table: 4.7 shows the Docking score, glide energy and grid box values of binding site of BSA with Alizarin. Higher the negative value of the docking score, better the binding affinity of the ligand and receptor [9]. The minimum energy for binding and higher number of hydrogen bonds also indicates good binding affinity of ligands towards the receptor. The docking score is -6.918.

The amino acid residues involved in the binding of AZ with BSA are predicted and their respective molecular distances from the drug have been presented in Table: 4.8. There are two hydrogen bonds between Alizarin and Glu353, H-O of bond length 1.35 A° and 1.62 A°. Figure: 4.7.3 shows the ligand interaction diagram of AZ and BSA. Fig: 4.9 shows the complex structure which indicates the amino acids involved in hydrogen bonding. By analyzing the binding site, docking score and other parameters from the docking results shows that AZ had a good binding affinity with BSA. Glide energy and the presence of hydrogen bonds in the binding mode reveals that Alizarin can be used as antitumor drug for cancer treatment.

Table 4.7: Docking score, glide energy and grid box values, potential energy, glide interaction efficiency of binding site of BSA with Alizarin

1	Docking score	-6.918
2	Glide gscore	-6.959
3	Glide energy	-26.085KCal/Mol
4	Grid box X cent	18.64
5	Grid box Y cent	18.38
6	Grid box Z cent	42.79
7	Potential energy	90.249 KJ/mol
8	Glide ligand efficiency	-0.384

TABLE 4.8: Atoms involved in the binding of AZ with BSA and the estimated distances between the protein and ligand atoms

PROTEIN ATOM	**LIGAND ATOM**	**DISTANCE (A°)**
Glu 353 C_{2720}=O_{2721}	O_{8646}-H_{8668}	1.62
Glu 353 C_{2720}=O_{2721}	O_{8643}-H_{8667}	1.35

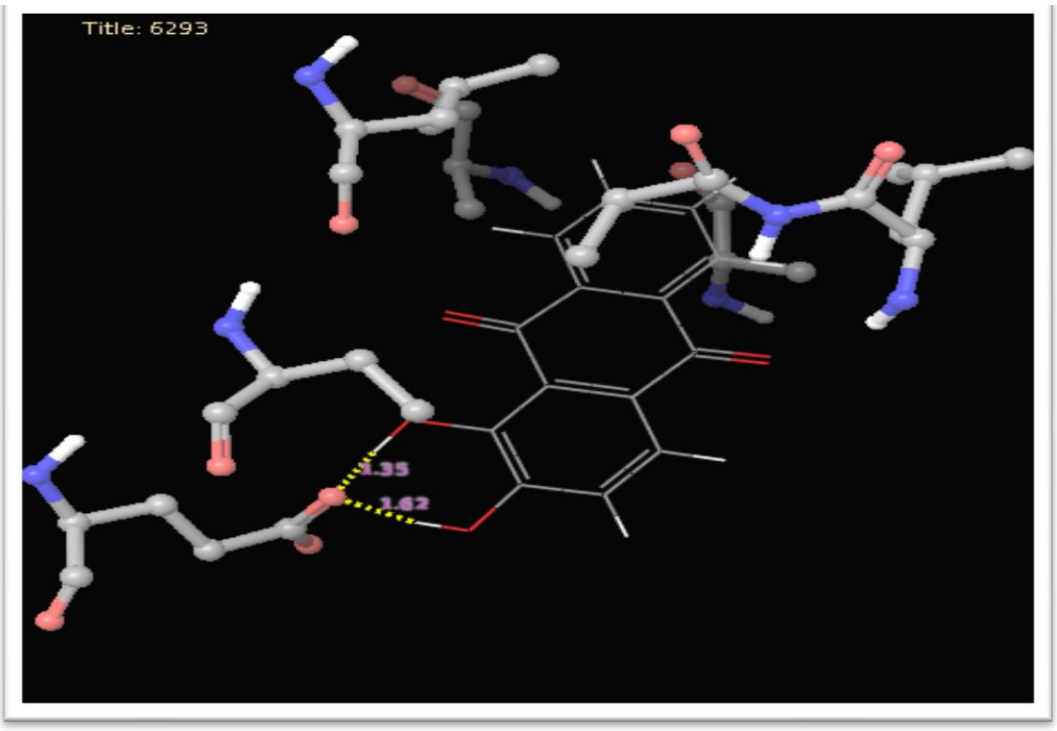

Fig: 4.9 shows the complex structure indicating the amino acids involved in hydrogen bonding.

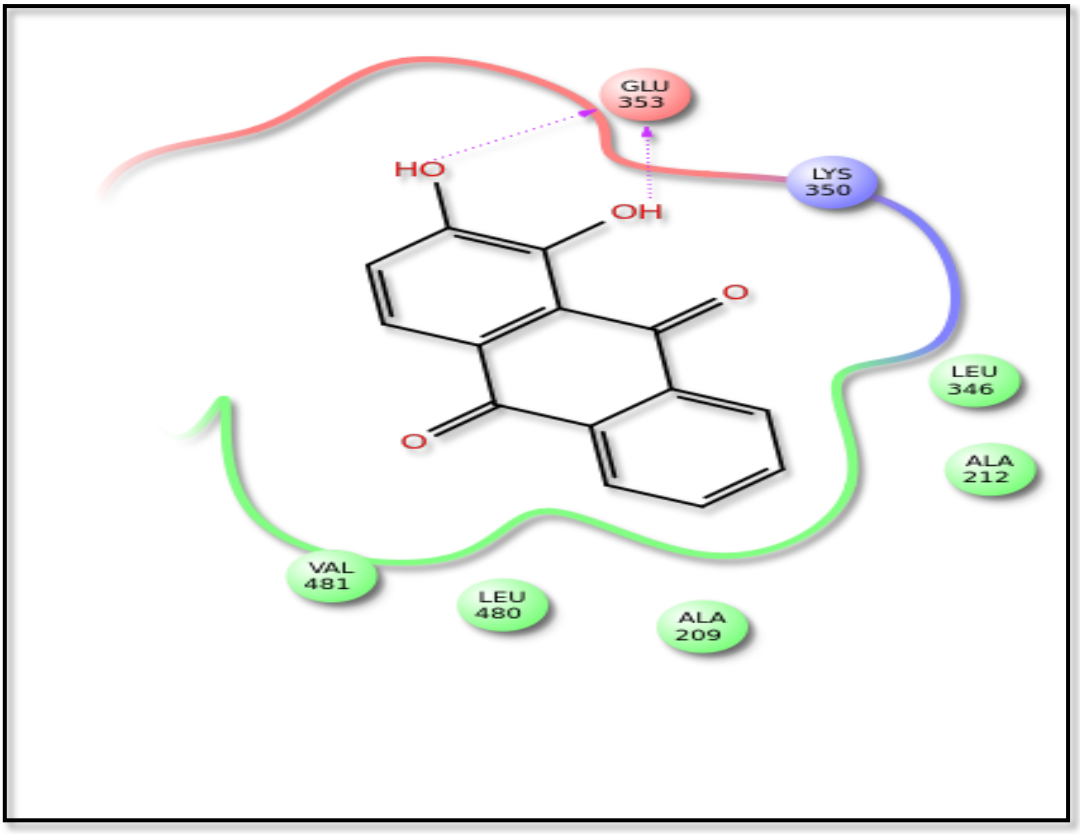

Fig: 4.10 Ligand Interaction Diagram of Alizarin With BSA

4.6 REFERENCES:

[1] A. Baran,a B. Wrzosek,b J. Bukowska,b L. M. Proniewicza andM. Baranskaa; Analysis of alizarin by surface-enhanced and FT-Raman spectroscopy; J. Raman Spectrosc. 2009, 40, 436–441.

[2] Anna Amat, Costanza Miliani, Aldo Romani and Simona Fantacci; DFT/TDDFT investigation on the UV-vis absorption and fluorescence properties of alizarin dye; Royal Society Of Chemistry; 2015, 17, 6374—6382.

[3] Dr. Sathyanarayana; Vibrational Spectroscopy- Theory and application; New age international publishers; 2001; pages 1.

[4] B.Z. Shakhashiri; Chemistry 103; 2009; pages 2850.

[5] T. Jayavarthanan, N. Sundaraganesan, M. Karabacak, M. Cinar , M. Kurt; Vibrational spectra, UV and NMR, first order hyperpolarizability and HOMO–LUMO analysis of 2-amino-4-chloro-6-methylpyrimidine; Spectrochimica Acta Part A: Molecular and Biomolecular Spectroscopy 97 (2012) 811–824.

[6] B.K.Sharma; spectroscopy; Krishna prakash media private limited; 2007; Pages: 250,251.

[7] M. Kandasamy, G. Velraj, S. Kalaichelvan; Vibrational spectra, NMR and HOMO–LUMO analysis of 9-fluorenone-2-carboxylic acid; Spectrochimica Acta Part A: Molecular and Biomolecular Spectroscopy 105 (2013) 176–183.

[8] A. Suvitha, S. Periand, M. Govindarajan, P. Gayathri; Vibrational analysis using FT-IR, FT-Raman spectra and HF–DFT methods and NBO, NLO, NMR, HOMO–LUMO, UV and electronic transitions studies on 2,2,4-trimethyl pentane; Spectrochimica Acta Part A: Molecular and Biomolecular Spectroscopy 138 (2015) 900–912.

[9] Kesavan, Priya Rramanathan, Rajkumar Thangarajan; Molecular modelling and docking studies of human acrosin binding protein (acrbp/oy-tes-1);Sabitha International Journal of Pharmacy and Pharmaceutical Sciences, Vol 7, Issue 9, 2015, pages 491-495.

SUMMARY AND CONCLUSION

CHAPTER V

SUMMARY AND CONCLUSION

The minimum energy structure of Alizarin and Alizarin in different solvents like Methanol (MeOH), DMSO, CCl_4 is obtained by using DFT method with B3LYP/ 6-311++ G (d,p) using Gaussian 09 package. Using the optimized structure, geometrical parameters like Bond length, Bond angle and Dihedral angle of Alizarin is determined by using the same level of theory. The fundamental vibrational frequencies and intensity of the vibrational bands of Alizarin is observed by using optimized structure in different solvents. Absorption spectra for AZ and AZ with different solvents are also obtained by TD-DFT method. The highest peak is obtained for Methanol 247.2nm and second highest peak is for vacuum 238.8nm. The ^{1}H and ^{13}C nuclear magnetic resonance (NMR) chemical shifts of AZ and AZ with different solvents were calculated by using the gauge independent atomic orbital method (GIAO) and the spectrums are also ploted. The highest isotropic chemical shift is for vacuum (C16=64.1172ppm, H26=27.5796ppm). Also Alizarin is docked with Bovine Serum Albumin (BSA). The docking studies are done by using the maestro/Glide of Schrödinger software, USA. The hydrogen bond interaction between AZ and BSA were studied.